

**Update of the water quality model  
application of the Schelde for the  
year 2014**

**Calibration and validation**





## **Update of the water quality model application of the Schelde for the year 2014**

**Calibration and validation**

Willem Stolte, Rudy Schueder

11203725

©Deltares, 2019



**Title**

Update of the water quality model application of the Schelde for the year 2014

<b>Client</b>	<b>Project</b>	<b>Reference</b>	<b>Pages</b>
Rijkswaterstaat	11203725	11203725-000-ZKS-0003	52

**Classification****Keywords**

Schelde, water quality, primary production, phytoplankton, SPM, light

**Summary**

Setup, calibration and validation is described for a 3D water quality and primary production model in the Schelde. The area of interest is the Westerschelde. Target variables primary production and dissolved oxygen concentration were reproduced well. Primary production in this area is limited by light which is caused by the high turbidity in this area. The model is going to be used to estimate the effect of changes in suspended sediment by human activities (such as dredging) or natural processes (changing run-off) on primary production. An additional research application will be to disentangle the different processes contributing to the daily variation in dissolved oxygen, to improve measurements of primary production.

**References**

Version	Date	Author	Initials	Review	Initials	Approval	Initials
1.0	2019-04-10	Stolte	WS	T. Troost	TT	D.J. Walstra	DJW

**Status**

final version



## Contents

<b>1</b>	<b>Introduction</b>	<b>1</b>
<b>2</b>	<b>Water quality data analysis</b>	<b>3</b>
2.1	Data sources and parameters . . . . .	3
2.2	Locations for water quality monitoring data for 2014 . . . . .	3
2.3	Covariation of dissolved substances with salinity . . . . .	7
2.4	Covariation of particulate substances with SPM . . . . .	9
2.5	Relationship between extinction of measured photosynthetically active radiation and measured variables. . . . .	9
2.6	Phytoplankton monitoring data . . . . .	10
<b>3</b>	<b>Model setup</b>	<b>15</b>
3.1	Grid and aggregation . . . . .	15
3.2	Hydrodynamics and water residence time . . . . .	15
3.3	Numerical integration and dispersion . . . . .	15
3.4	Model observation points . . . . .	15
3.5	Boundary conditions . . . . .	18
3.6	Meteo input . . . . .	21
3.7	Substances and processes . . . . .	21
3.8	Primary production by phytoplankton . . . . .	22
3.9	Phytobenthos . . . . .	24
3.10	Grazing by zooplankton . . . . .	24
3.11	Grazing by macrozoobenthos . . . . .	24
<b>4</b>	<b>Results</b>	<b>25</b>
4.1	Salinity and total nutrients . . . . .	25
4.2	Inorganic nutrients . . . . .	28
4.3	Suspended sediments (SPM), light extinction coefficient (E), dissolved organic matter (DOC) and chlorophyll-a (Chlfa) . . . . .	28
4.4	Limiting factors for phytoplankton production and biomass . . . . .	30
4.5	Calibration and validation rationale . . . . .	30
4.6	Calibration of DOC light extinction coefficient . . . . .	31
4.7	Calibration by change of phytoplankton growth parameters . . . . .	31
4.8	Comparison of modelled and measured primary production . . . . .	34
4.9	Phytoplankton groups and biomass . . . . .	35
4.10	Dissolved oxygen . . . . .	35
4.11	Comparison with remote sensing data . . . . .	37
<b>5</b>	<b>Conclusions</b>	<b>39</b>
5.1	Performance of the model in relation to the target variables . . . . .	39
5.2	Uncertainties . . . . .	40
5.3	Recommendations for further development . . . . .	41
	<b>Appendix</b>	<b>43</b>
	Processes included in the model . . . . .	43
	Methodology for estimation of light extinction coefficients by DOC and SPM . . . . .	43
	<b>References</b>	<b>51</b>





## List of Figures

2.1	Number of water quality data lines per year and source . . . . .	4
2.2	Monitoring locations for water quality used in this study. The size of the station is indicative for the number of observations in 2014 . . . . .	4
2.3	Concentrations of dissolved substances in time. The stations are ordered from low mean salinity (left) to high mean salinity (right) . . . . .	5
2.4	Concentrations of dissolved substances in relation to salinity for the year 2014. . . . .	8
2.5	Concentrations of particulate bound substances in relation to suspended matter. . . . .	9
2.6	Biomass of different ecotypes phytoplankton in mgC/l . . . . .	11
2.7	Biomass of different taxonomic groups phytoplankton in mgC/l . . . . .	11
2.8	Total phytoplankton biomass at the three mwtl locations in the Westerschelde from 1990 - 2014. . . . .	12
2.9	Diatom biomass as a percentage of total phytoplankton biomass at the three mwtl locations in the Westerschelde from 1990 - 2014. . . . .	13
2.10	Carbon to chlorophyll ratio (g/g) during the model year 2014 in the Westerschelde. . . . .	13
2.11	Long term evolution of carbon to chlorophyll ratio (g/g) in phytoplankton in the Westerschelde. . . . .	14
3.1	Outline of the water quality and primary production model grid. . . . .	16
3.2	Aggregated grid for water quality and primary production model, indicating the spatial scale of segments in different parts of the grid. . . . .	16
3.3	A detail of the grid shows the differential aggregation of segments in the horizontal direction . . . . .	17
3.4	Age of water in the Westerschelde part of the model grid as calculated by the hydrodynamic model 3rd April 2014 . . . . .	17
3.5	Seaward boundary of the model grid, with boundary names (blue) and measurement locations used to compose the water quality boundary conditions. . . . .	18
3.6	Concentrations of relevant substances at the model sea boundary. . . . .	19
3.7	Correlations of dissolved substances with salinity per season in 2014. The freshwater boundary concentration was based on the extrapolation values of the substances to salinity = 0 promille for the different seasons. . . . .	20
3.8	Wind speed at Vlissingen in m/s. hourly values (grey) weekly running means (black) . . . . .	21
3.9	Irradiation at Vlissingen in J/cm <sup>2</sup> . Hourly values (grey) weekly running means (black) . . . . .	22
3.10	Forced potential biomass of zooplankton in the model, based on measurements . . . . .	24
4.1	Model-data comparison for salinity and total nutrient concentration at the MWTL monitoring stations for the uncalibrated model . . . . .	26
4.2	Target diagram for model performance: salinity, total nitrogen and total phosphorus . . . . .	26
4.3	Model-data comparison for inorganic nutrients at the MWTL monitoring stations for the uncalibrated model . . . . .	27
4.4	Target model performance diagram for inorganic nutrients at the MWTL monitoring stations for the uncalibrated model . . . . .	27
4.5	Model-data comparison for SPM, E, DOC, and Chlfa at the MWTL monitoring stations for the uncalibrated model . . . . .	29
4.6	Target model performance diagram for SPM, E, DOC, and Chlfa at the MWTL monitoring stations for the uncalibrated model . . . . .	29

# Deltares

4.7	Strength of limiting factor for diatom growth in the top layer as compared to chlorophyll a biomass before calibration. The thickness of the colored bands is indicative for the relative limitation by that factor . . . . .	30
4.8	Limiting factors in the second layer . . . . .	30
4.9	Model-data comparison for SPM, E, DOC, and Chlfa at the MWTL monitoring stations after lowering the specific extinction coefficient for DOC . . . . .	32
4.10	Target diagram for SPM, E, DOC, and Chlfa at the MWTL monitoring stations after lowering the specific extinction coefficient for DOC . . . . .	32
4.11	Modelled (line) and observed (dots) SPM, Extinction coefficient E, DOC, and Chlorophyll a for the model calibration run with decreased extinction coefficient for DOC and decreased mortality rate for diatoms and non-diatoms. . . . .	33
4.12	Target diagrams for the model calibration run with decreased extinction coefficient for DOC and decreased mortality rates. . . . .	33
4.13	Observed and modelled depth integrated primary production (top), chlorophyll-a during production measurements (middle), and specific primary production as gC/mgChlfa/day (bottom) at station Hansweert Geul. Observations from 2014 were not available for stations in the Westerschelde. Data were kindly provided by Dr. Jacco Kromkamp, Royal Netherlands Institute for Sea Research (NIOZ). . . . .	34
4.14	Model - observation comparison for phytoplankton biomass in carbon for the model calibration with 1. decreased extinction coefficient for DOC, and 2. decreased mortality of the diatoms and non-diatoms. . . . .	35
4.15	Target diagrams for phytoplankton biomass in carbon for the model calibration with 1. decreased extinction coefficient for DOC, and 2. decreased mortality of the diatoms and non-diatoms. . . . .	35
4.16	Modelled (line) and observed (dots) dissolved oxygen for the model calibration with 1. decreased extinction coefficient for DOC, and 2. decreased mortality of the diatoms and non-diatoms. . . . .	36
4.17	Target diagrams of model-observation comparison of dissolved oxygen for run 33. . . . .	36
4.18	Saturation of dissolved oxygen dependent on salinity and temperature. From: Fondriest Environmental, Inc. "Dissolved Oxygen." Fundamentals of Environmental Measurements. 19 Nov. 2013. [weblink]( <a href="https://www.fondriest.com/environmental-measurements/parameters/water-quality/dissolved-oxygen/">https://www.fondriest.com/environmental-measurements/parameters/water-quality/dissolved-oxygen/</a> ) . . . . .	36
4.19	Modelled (line) and observed (dots) temperature for the model calibration with 1. decreased extinction coefficient for DOC, and 2. decreased mortality of the diatoms and non-diatoms. . . . .	36
4.20	Target diagrams of model-observation comparison of dissolved oxygen for run 33. . . . .	37
4.21	Modelled (line) diurnal patterns (2 days in beginning of May) of dissolved oxygen for the model calibration with 1. decreased extinction coefficient for DOC, and 2. decreased mortality of the diatoms and non-diatoms. . . . .	37
4.22	Comparison of SPM between model, in situ data and remote sensing derived information. . . . .	37
5.1	Correlation between parameters per year . . . . .	44
5.2	Correlation between parameters per station . . . . .	45
5.3	LEAPS plot showing the r-squared of the multiple regression against the number of variables used. The text in the plot indicates which variables are used for each value of r-squared . . . . .	47
5.4	Observed vs predicted E according to model 3. The model year 2014 is plotted on top of the other years in higher opacity. Larger sized symbols represent relatively fresh water stations. . . . .	49

## List of Tables

3.1	Estimated concentrations for upstream boundaries . . . . .	21
3.2	List of substances (state variables) used in the model. . . . .	23
5.1	Table with all active processes used in the Schelde water quality and primary production model . . . . .	46
5.2	. . . . .	48



## 1 Introduction

The Schelde estuary has been recovering from severe nutrient pollution and oxygen deficiency (T. J. S. Cox et al. (2009) P. Meire et al. (2005)). Still, it is heavily influenced by human activities, directed to safety, transport, and natural resources. This causes pressures on the natural habitats in the Schelde and its shores. Understanding the natural processes and how they are influenced by human activities is essential for management of the Schelde estuary.

Primary production by pelagic and benthic algae is the energetic basis of the natural habitats in any marine ecosystem. In the Schelde, pelagic primary production is strongly limited by the amount of available light (Spaendonk (1993), J. Kromkamp et al. (1995)) due to the high concentrations of suspended sediments.

Pelagic primary production results in phytoplankton biomass, but the ambient concentration of phytoplankton depends heavily on the residence time of a water parcel in favourable conditions, as well as loss terms such as grazing by zooplankton and benthic filter feeders. It is therefore difficult to estimate primary production from standing stock phytoplankton biomass or, even more difficult, from chlorophyll-a. Still, these types of biomass measurements form the basis for many assessments and management decisions. Production measurements are done, but usually more limited in time and space. A model gives a possibility to test our knowledge on processes relating suspended sediment, light, primary production and phytoplankton standing stock.

This report describes an update of the water quality and primary production model for the Schelde. The previous model was set up to simulate the year 2006 (Van Kessel et al. 2011). The current model is simulating the year 2014. It builds on a hydrodynamic model developed by WL Borgerhout, Antwerpen, Belgium for transport of water and dissolved and suspended substances (for description, see also Cronin and van Kessel (2018)). A separate sediment model (Cronin and van Kessel (2018)) has been developed in concert, and suspended sediment output of that model is used as a forcing function in the current primary production model.

To objectively estimate the consequences of morphological and/or sediment transport processes for primary production in the Westerschelde, a spatially explicit model is necessary. With the use of such a model, an objective prediction can be made of changes in primary production as a result of changing suspended sediment concentrations from activities such as dredging. As such, a water quality and primary production model will work in concert with the sediment model.

There are already models available that predict primary production in the Schelde/Westerschelde. These are:

- MOSES model of the Schelde (Soetaert1995 and developments hereafter), simulating multiple years in a 1-D horizontal schematization. The model can be used to predict primary production as a result of environmental conditions in the Schelde on the scale of segments with a size of appr km. The high level of aggregation results in a robust and fast model with which many scenarios or sensitivity analyses can be run. However, the spatial scale does not facilitate scenarios concerning e.g. dredging plumes. Also, suspended sediment is a forcing function, and is not recalculated by the model.
- Delft3D water quality (Delwaq) model simulating the year 2006. This model calculates primary production on a 3D fine-scale (0.5 to 2 km) schematization. This model is suitable to predict changes in primary production as a result of changing environmental conditions

(e.g. suspended sediment) on a fine scale. Suspended sediment can be recalculated by the accompanying sediment model.

The latter model is suitable for many types of scenarios, but is outdated (year 2006). Also, the model did not produce accurate simulations of phytoplankton biomass/production over the whole area of interest (Westerschelde). Typically, at the upstream side of the Westerschelde, the phytoplankton spring bloom was overestimated while its biomass was underestimated during the summer.

The aim of this study is therefore to construct, calibrate and validate a model that simulates the target variable primary production in the Schelde as a function of environmental conditions, most notably the suspended sediment concentration field in the estuary. The area of most interest is the Dutch part of the estuary, Westerschelde, roughly between the Dutch-Belgian border and the mouth of the estuary. The model suitability for scenarios is discussed.

The target variables are

- primary production over the Westerschelde area. The model will be judged by its performance to reproduce primary production during a growth season (hindcast).
- Variation in dissolved oxygen concentration in order to compare to a Belgian study on calculation of primary production from variation in dissolved oxygen concentration (Tom J. S. Cox et al. (2015))

The rest of the report is structured as follows:

- As a first step in the model construction, the input and validation data for the model will be shortly analyzed. The knowledge of the analysis is used in the model construction and calibration.
- The setup of the updated model is described
- The initial results are shown
- The results of calibration steps and the results of the final product are presented
- The results are discussed in the light of the data analysis, and consequences for the usability of the model are presented.

## 2 Water quality data analysis

An interactive tool for data exploration of water quality time series for the Schelde has been made available at <http://al-ng036.xtr.deltares.nl/deltares/interactivescheldt/>

### 2.1 Data sources and parameters

Observations for 2014 were obtained from two different data sources. Since the area of interest is the Westerschelde, only stations downstream of Antwerpen were considered in the calibration/validation of the model.

- The Scheldemonitor data portal - This is a combination of Dutch and Flemish data covering the freshwater part and the marine part up to Vlissingen. Also, it contains data at two North Sea stations in the vicinity of the grid. (<http://www.scheldemonitor.be/dataproducts/nl/download/>).
- The MUMM data portal - These data cover Flemish data from the North Sea part of the grid and just outside the grid.

The Dutch “Waterbase” portal (<http://live.waterbase.nl> and copy at <http://opendap.openearth.deltares.nl>) also contains water quality data for the Dutch part of the Schelde. However, after checking, it was concluded that all relevant Waterbase data for the year 2014 already were included in the Scheldemonitor data.

From the MUMM database, in total 270 observations were extracted, and 2069 from the Scheldemonitor for the year 2014, which is much lower than e.g. for the period 1995-2010 (figure 2.1).

### 2.2 Locations for water quality monitoring data for 2014

For 2014, biweekly water quality observations were available from Scheldemonitor in the Westerschelde. These measurements are done in the scope of the Dutch long-term monitoring program MWTL. From MUMM, observations from the coastal zone were available at a lower frequency (figure 2.2).

Concentrations of relevant water quality parameters in 2014 (see figure 2.3) are plotted for the most important stations. Nutrient concentrations show a decreasing trend from Schaar van Ouden Doel (Belgian border) to the North Sea. There are strong seasonal patterns for DIN, PO<sub>4</sub> and SiO<sub>2</sub> due to algal production in the estuary. Dutch MWTL stations were sampled more frequent than the Belgian MUMM Stations in this area, but concentrations were similar. The high concentration of Chlorophyll-a at Schaar van Ouden Doel is probably caused by phytoplankton that is extremely adapted to low light in this area. NH<sub>4</sub> and PO<sub>4</sub> at Schaar van Ouden Doel show increased concentrations in summer, possibly due to remineralization which is temperature dependent. This was not seen at the other stations. The variation in DOC concentrations can be explained by variation in river discharge which is lower during summer.

The variations of substances is mainly due to two different mechanisms:

1. transport and mixing are causing dilution of nutrients by seawater. This causes an inverse linear relationship with salinity.
2. processes, like uptake of nutrients by phytoplankton, remineralization in the sediment, or sorption by suspended particulate matter contribute to deviations from the above mentioned linear relationship.

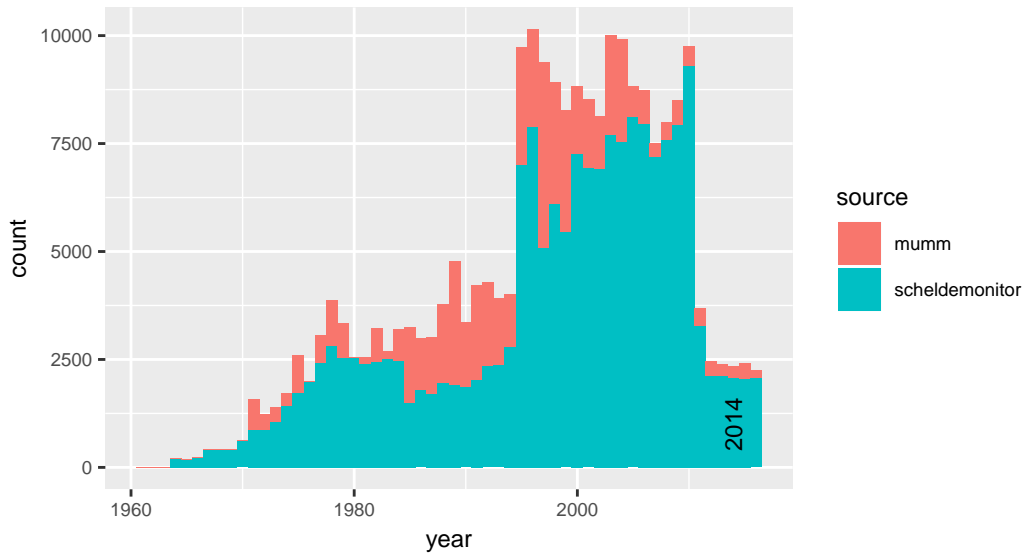


**Figure 2.1:** Number of water quality data lines per year and source

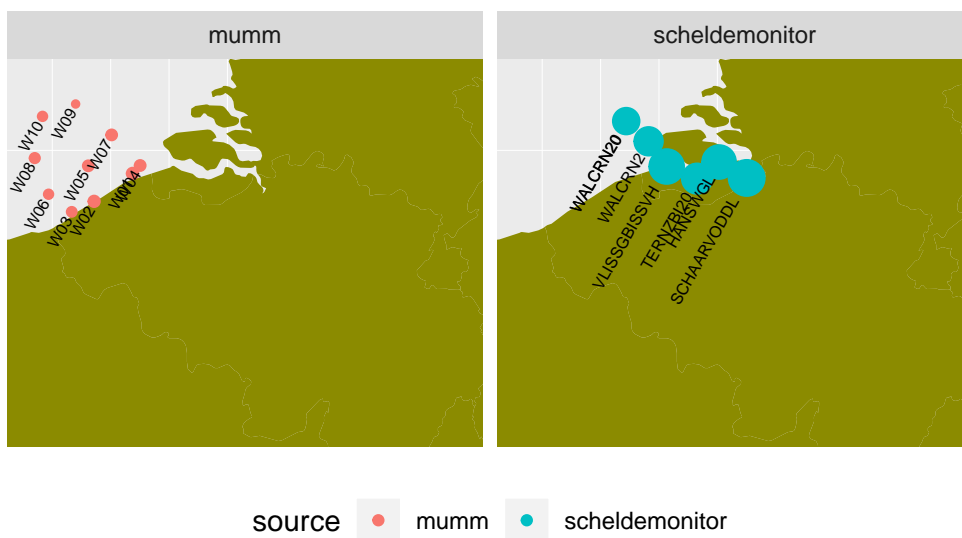


**Figure 2.2:** Monitoring locations for water quality used in this study. The size of the station is indicative for the number of observations in 2014



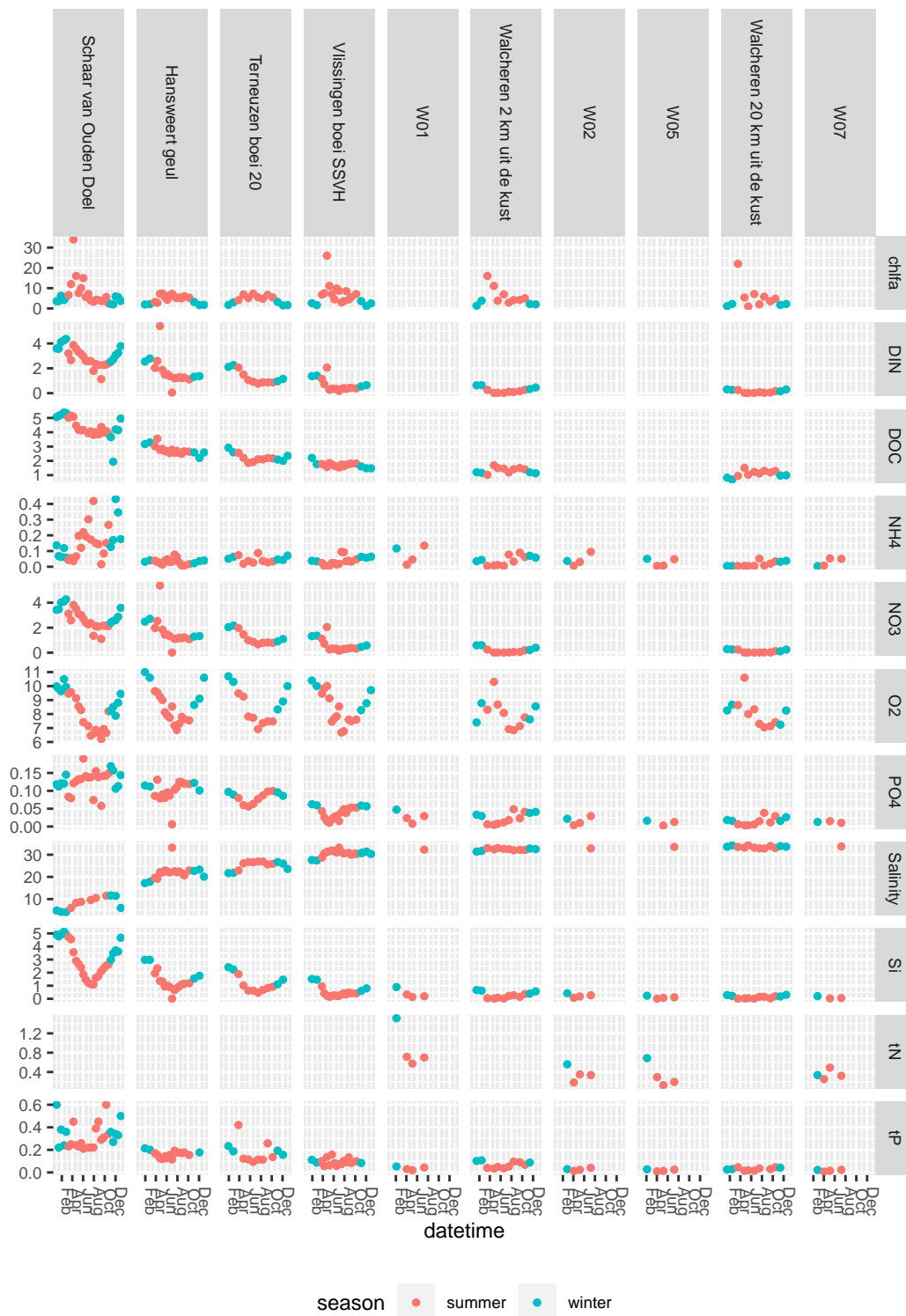


**Figure 2.3:** Concentrations of dissolved substances in time. The stations are ordered from low mean salinity (left) to high mean salinity (right)

To understand better the relative contribution of these different mechanisms, the relationship of substances with salinity and SPM were made.

### 2.3 Covariation of dissolved substances with salinity

For selected parameters, the variation with salinity for 2014 was plotted (figure 2.4). If no processes occur, and in the absence of other major sources or sinks, dissolved substances originating from land, such as nutrients, will be inversely proportional to salinity. Deviations to this pattern indicate variability in loads, (seasonal) processes, or major sinks to or sources from e.g. the sediment, polders, etc. (figure 2.4)

Summer values represent monitoring results from March - October; winter values from November - February.

Nitrate ( $\text{NO}_3$ ) concentrations are dominated by dilution rather than processes, as the concentration decreases linearly with salinity. Apparently, uptake by phytoplankton and bacterial processes (nitrification and denitrification) do not have a strong effect on nitrate concentrations in the water. Total dissolved inorganic nitrogen (DIN,  $\text{NO}_3 + \text{NO}_2 + \text{NH}_4$ ) behaves similar, because most of DIN is in the form of  $\text{NO}_3$ . The small difference between summer and winter values suggest that no substantial part of the DIN is used for primary production.

Ammonium ( $\text{NH}_4$ ) concentration does not show a strong relationship with salinity. Its variation is likely more dominated by processes in the water or sediment, as well as by external sources.

Chlorophyll a (chlfa) concentrations did not show any trend with salinity, which can be expected, as phytoplankton biomass is strongly regulated by local processes. Typical concentration in the summer of 2014 is around 5 to 10  $\mu\text{g}/\text{l}$ , comparable to what has been found earlier [Kromkamp1995a]. Winter concentrations are lower. At 10 psu salinity, high concentrations occur during summer at Schaar van Ouden Doel.

Dissolved organic carbon (DOC) concentration shows a strong and linear relation with salinity, indicating that most of DOC is “passing by”, i.e. not subject to any production or degradation in this part of the Schelde. For this reason, it is likely that this DOC consists merely of stable humic-like substances.

Dissolved oxygen does not show a clear relation with salinity. This is expected because it is in continuous equilibrium with the atmosphere. The low concentrations at 10 psu salinity during summer occurs at Schaar van Ouden Doel and coincides with high chlorophyll and low dissolved silicate.

Dissolved phosphate concentration ( $\text{PO}_4$ ) is highest at 10-15 PSU salinity, indicating a source of  $\text{PO}_4$  at that salinity. This could be caused by redelivery of  $\text{PO}_4$  from the sediment, or an other source from land. The small difference between summer and winter values suggest that no substantial part of the  $\text{PO}_4$  is used for primary production.

Winter concentrations of dissolved silicate (Si) seem to correlate well with salinity. However, in summer, a distinct reduction of Si is seen as compared to winter concentrations. This can be explained by growth of diatoms in the fresh part of the river, taking up a substantial part of the Si.



**Figure 2.4:** Concentrations of dissolved substances in relation to salinity for the year 2014.

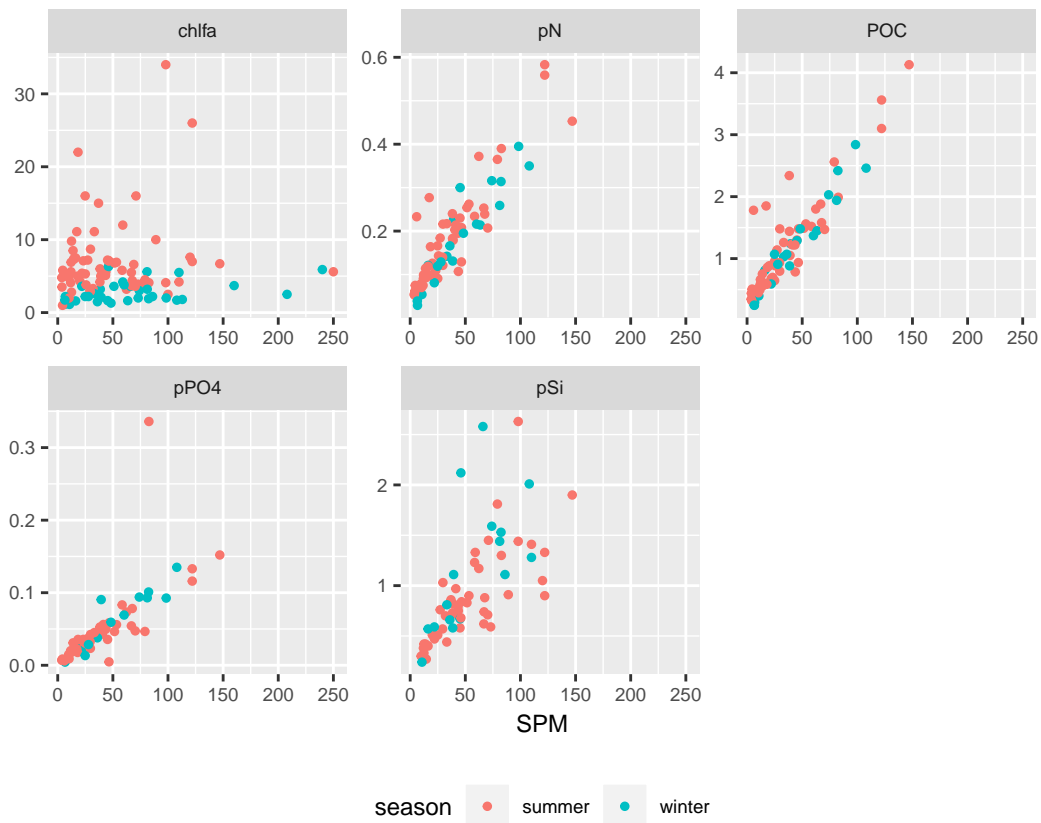


**Figure 2.5:** Concentrations of particulate bound substances in relation to suspended matter.

#### 2.4 Covariation of particulate substances with SPM

Particulate nitrogen, phosphorus, Silica and carbon were highly correlated with the concentration of SPM and did not vary much between summer and winter (figure 2.5). The concentration of Chlorophyll-a did not correlate not very clearly with SPM. A negative correlation could be expected, because SPM reduces the penetration of light in the water column. On the other hand, phytoplankton growth and biomass are highest in summer, irrespective of SPM concentration. A complicating factor is that phytoplankton produce more chlorophyll-a in dark circumstances, so at high SPM concentrations. The interaction between these processes is that there is no clear relation visible.

#### 2.5 Relationship between extinction of measured photosynthetically active radiation and measured variables.

For modelling of primary production, correct estimation of underwater light climate is essential. Different models exist to explain the underwater light climate. An important ingredient in all models is the extinction coefficient ( $E$ ), describing the exponential decrease of apparent available light with depth according to the Lambert-Beer equation:

$$I_d = I_0 * e^{-E*d}$$

where  $I_d$  is the irradiance at depth  $d$ ,  $I_0$  is the irradiance just below the surface and  $E$  is the extinction coefficient.

In the model used in this study, the extinction coefficient  $E$  depends on the concentrations of substances that absorb light, and their respective absorption coefficient, resulting in:

$$E = a + b * TIM + c * DOC + d * POC + f * CHLFA$$

where  $a$  is the background extinction (0.08 in Delft3D WAQ), and  $b$ ,  $c$ ,  $d$  and  $f$  the specific extinction coefficients for TIM (total inorganic matter), DOC (dissolved organic matter), POC (particulate organic matter) and CHLFA respectively.

The total extinction coefficient  $E$  is measured at the three MWTL stations in the Westerschelde (Dutch part of the estuary). Using the equation and the concentrations of the different compounds, an estimate of the coefficients was made by multiple regression.

Based on testing (see Appendix), the following model was used to for explaining  $E$  based on field measurements:

$$E = a + b * SPM + c * DOC + d * CHLFA$$

POC was not taken into the equation, because it is included in the measured SPM.

The conclusion of a multiple regression analysis was that the constants were not significantly different from the normally used default values that are used for marine waters. Default values were therefore applied for the initial model setup. These are:

Default values for coefficients are:

constant ( $a$ ): 0.08 (background extinction of water)

spm ( $b$ ): 0.022

DOC ( $c$ ): 0.393

chlfa ( $d$ ): 0.006

The analysis also reveals that this estimation tends to underestimate  $E$  at low values of  $E$  (low concentrations of DOC and SPM) and overestimates  $E$  at very high values of  $E$ .

## 2.6 Phytoplankton monitoring data

Phytoplankton data were obtained from the servicedesk data at Rijkswaterstaat (servicedesk-data-at-rws.nl). Classification into groups was done using extra metadata provided by the analysing bureau via Rijkswaterstaat.

Normally, marine species dominated the population of phytoplankton. Only in the beginning of the year 2014, at station Schaar van Ouden Doel, freshwater species comprised approximately equal biomass as marine species (figure 2.6).

Taxonomically, diatoms were the dominating group of phytoplankton, except at the start of 2014 at station Schaar van Ouden Doel (figure 2.7). It is clear that there is no clear spring bloom at Schaar van Ouden Doel and Hansweer Geul. At Vlissingen, the spring bloom is followed by a longer period of increased biomass. Also, there is a short peak of Phaeocystis following the diatom spring bloom. Apparently, there is no nutrient depletion, and phytoplankton is not controlled strongly by grazing.

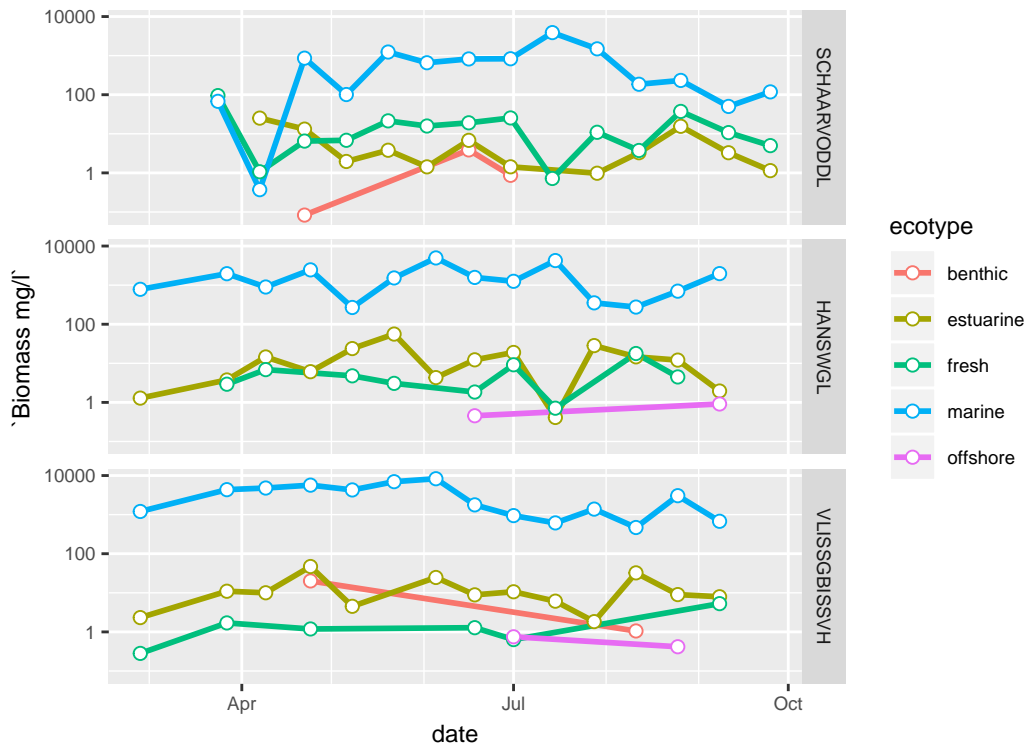


Figure 2.6: Biomass of different ecotypes phytoplankton in mgC/l

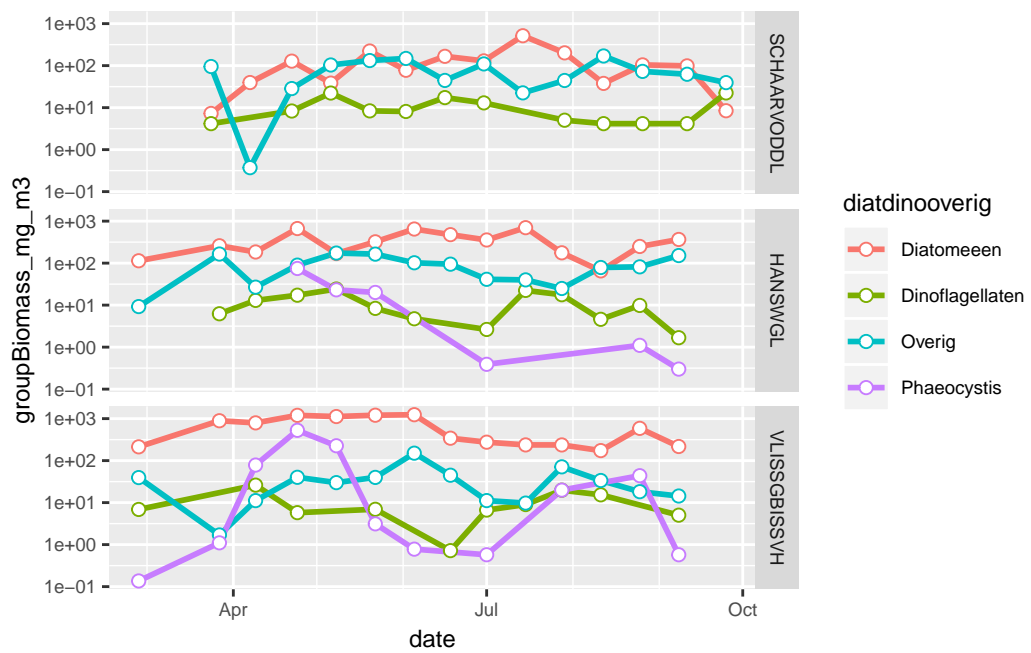
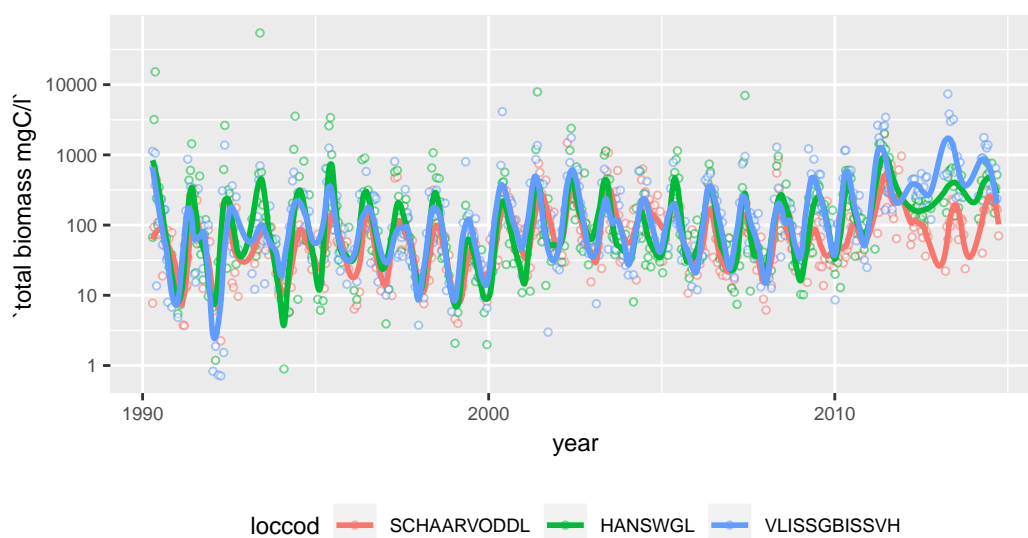


Figure 2.7: Biomass of different taxonomic groups phytoplankton in mgC/l



**Figure 2.8:** Total phytoplankton biomass at the three mwtl locations in the Westerschelde from 1990 - 2014.

Long term phytoplankton biomass development is shown in figure 2.8. Total biomass increased in general over this period. Especially at the stations Hansweert Geul and Vlissingen phytoplankton biomass has increased from 2011 on average. In 2015, only Phaeocystis was counted, which is not shown here.

While the total biomass increased from 1990 to 2000, the fraction of diatoms decreased, mostly at Schaar van Ouden Doel. From 2000, diatom fraction has stabilized to a level lower than at the beginning of the 1990's (figure 2.9).

Observed phytoplankton carbon to chlorophyll ratios were calculated using the total biomass of phytoplankton from phytoplankton cell counts, and the measured concentrations of chlorophyll-a at the same date and location. The station Schaar van Ouden Doel, at salinities of around 10 PSU, expressed very low carbon per chlorophyll. At the rest of the stations, the ratio was around 50 to 100 (indicating that chlorophyll a mass is 1 - 2 % of the carbon biomass) or even higher (2.10). It can be expected that the chlorophyll content is high (and C/Chlfa low) in environments with less light. However, values below 25 g/g (green line in the figure) are considered low and below 10 as extremely low (Cloern et al. (1995), Wang and Wu (2009)), indicating strong and extreme light limitation respectively. In the North Sea, C/Chlfa varied from 10 as lowest values in the coastal zone to 200 in offshore waters (Alvarez-Fernandez and Riegman (2014)).

Very low C/Chlfa values are found in early spring at Schaar van Ouden Doel, which indicates extreme light limitation (figure 2.10). Care has to be taken when calibrating the model results as chlorophyll-a at this station for the spring period, since the chosen algal module in this version of the model does not include variable C/Chlfa ratio's. In any case, the value of C/Chlfa close to 1 unrealistic. This could be due to chlorophyll-a determination, phytoplankton biomass estimation, or to variation because of patchiness during sampling.

Historically, C/Chlfa ratio's have been very low at all three stations (figure 2.11). Before 2010, moving average C/Chlfa ratio's are lower than 25. This means that during that period, the Westerschelde was dominated by strong light limiting conditions. At present time, light limitation is weaker, or even relieved at the stations Hansweert Geul and Vlissingen. At Schaar van





**Figure 2.9:** Diatom biomass as a percentage of total phytoplankton biomass at the three mwtl locations in the Westerschelde from 1990 - 2014.

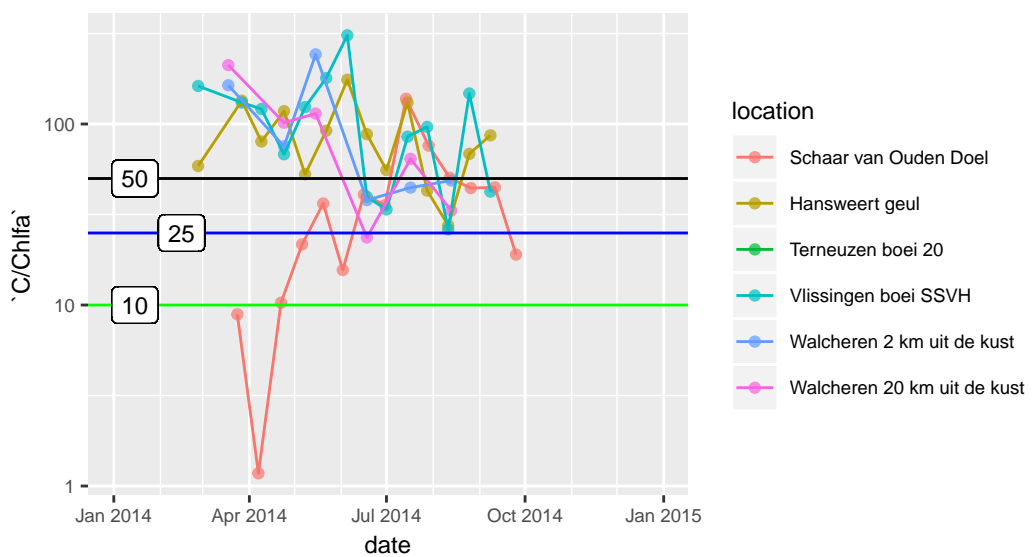


**Figure 2.10:** Carbon to chlorophyll ratio (g/g) during the nmodel year 2014 in the Westerschelde.

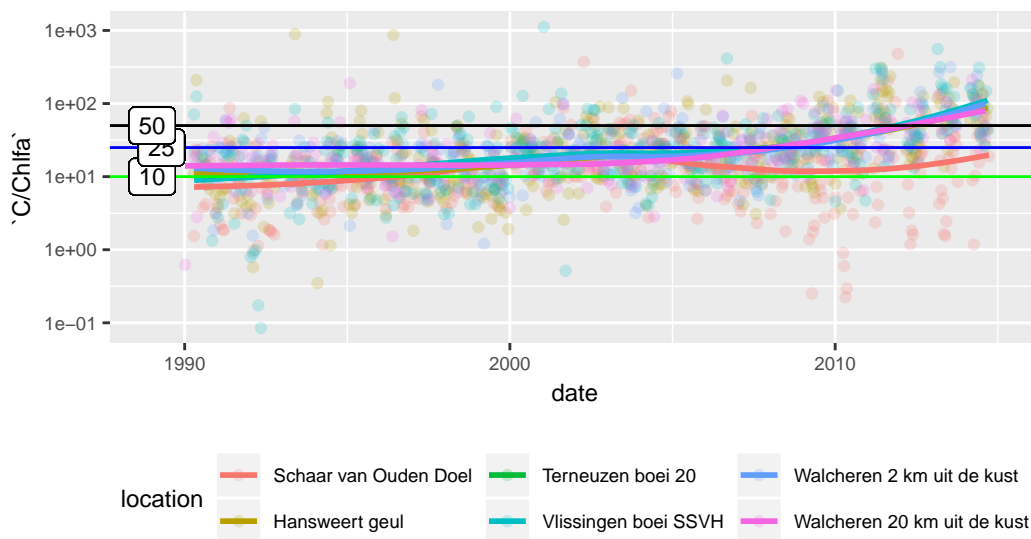


**Figure 2.11:** Long term evolution of carbon to chlorophyll ratio (g/g) in phytoplankton in the Westerschelde.

Ouden Doel, there seems to be strong light limitation during the whole period.

To summarize:

- Schelde contains high concentrations of suspended matter and DOC, that both contribute to the attenuation of light.
- Nutrient concentrations are high. The variation in nutrient concentration over the whole model domain is more driven by transport and mixing than by processes. Locally in the Westerschelde, nutrient concentrations show seasonal patterns caused by uptake by algae.
- Phytoplankton in the Westerschelde are generally dominated by marine species. Only at the onset of 2014, when high river discharge occurred, freshwater species were equally important, but at very low abundance. Therefore, there is no need to define separate freshwater and marine species.
- The chlorophyll to carbon ratio in the Westerschelde varies from ~10 in early spring at Schaar van Ouden Doel, to over 100 during summer at the mouth of the estuary. This should be taken into account when calibrating/validating on chlorophyll-a concentration.
- The proportion of diatoms in the Westerschelde, especially at Schaar van Ouden Doel has decreased over the past decades.

## 3 Model setup

The model presented here is preceded by a similar model forced with hydrodynamics, suspended sediments and environmental from the year 2006 (Stolte and van Oorschot 2012). The main conclusions from the calibration and validation were that yearly primary production was estimated correctly, but not the timing of blooms. The model was used in scenario studies concerning the enhanced fresh water inflow at Bath (Bathse Spuisluizen) (Chatelain & Van Duren, 2015). In the scenario study, improvements were made with respect to simulation of phytoplankton as compared to the initial model.

### 3.1 Grid and aggregation

The water quality model application builds on the hydrodynamic model application by the Flemish institute Borgerhout (version 'SDS-NEVLA3D2014' (figure 3.1). The hydrodynamic model grid consists 200194 horizontal segments and 6 z-layers (1201164 segments in total).

For water quality calculation, this is a high number of segments that will slow down calculations considerably. Also, not the same spatial detail is needed for water quality as for hydrodynamic calculations. The grid was therefore aggregated horizontally (figure 3.3), taken into account that the vertical resolution is needed to resolve the variability of salinity in combination with the strong horizontal movement of the water due to tides.

Consistent with the earlier version of the WQ model, horizontal aggregation was performed as a 4x4 aggregation in shallow areas (<5m NAP) and 16x16 in deeper areas (>5m). The resulting grid consist of just under 1000 segments for each vertical layer.

### 3.2 Hydrodynamics and water residence time

The hydrodynamic model produced, after aggregation, the water transport for the water quality and primary production model. The model is described in detail elsewhere (Cronin and van Kessel (2018)). For water quality and primary production, the residence time of the water is important for the resulting concentrations of e.g. phytoplankton biomass. A tracer sum was done to check the calculated water age in the model grid area.

It appears that the area with highest residence time is in the Westerschelde.

### 3.3 Numerical integration and dispersion

Numerical option nr 21 in the D-Water Quality software has been used. This is a combination of explicit and implicit integration methods, depending on stability criteria (DWAQ manual, section 10.5)

### 3.4 Model observation points

Observation points are assigned to the segments in layer 1, because monitoring observations were all from the surface layer (1 m depth) and were defined by intersection of their coordinates with the waq grid. All water quality monitoring locations were included in the model, and some additional points were added for better model understanding.

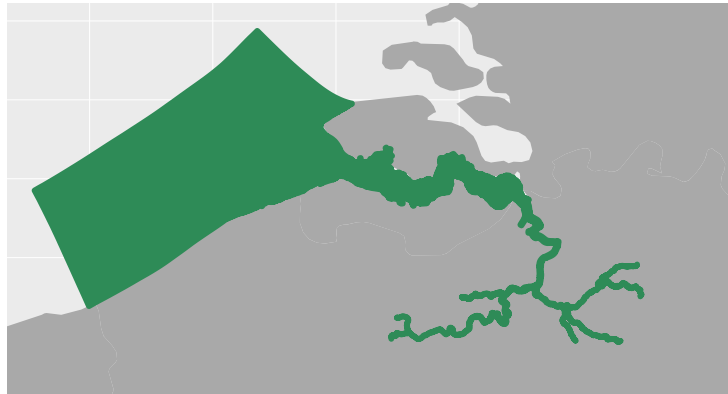


**Figure 3.1:** Outline of the water quality and primary production model grid.

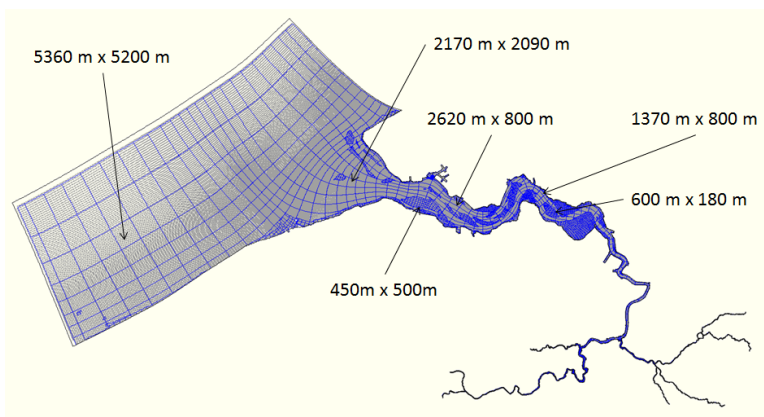


**Figure 3.2:** Aggregated grid for water quality and primary production model, indicating the spatial scale of segments in different parts of the grid.

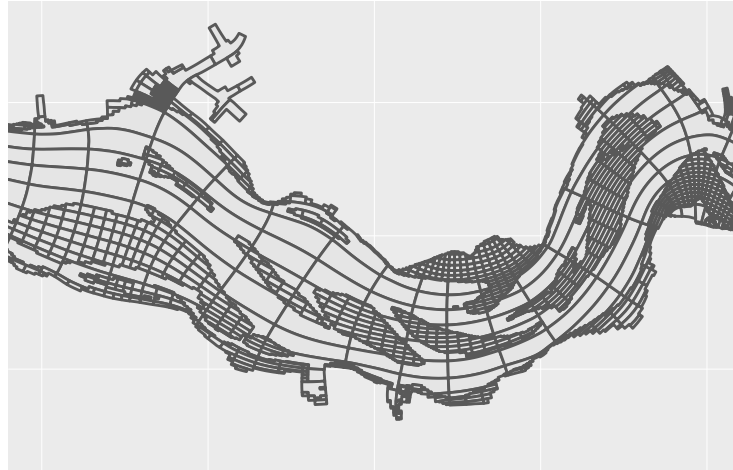


**Figure 3.3:** A detail of the grid shows the differential aggregation of segments in the horizontal direction

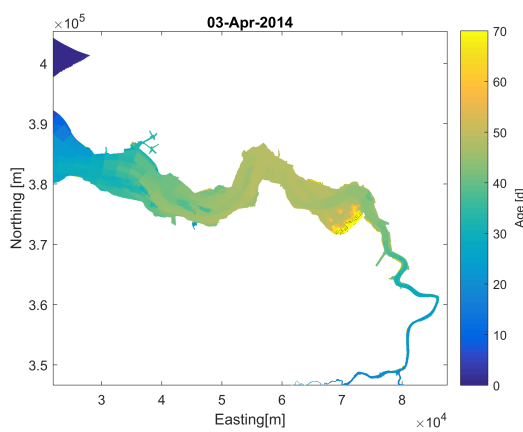


**Figure 3.4:** Age of water in the Westerschelde part of the model grid as calculated by the hydrodynamic model 3rd April 2014

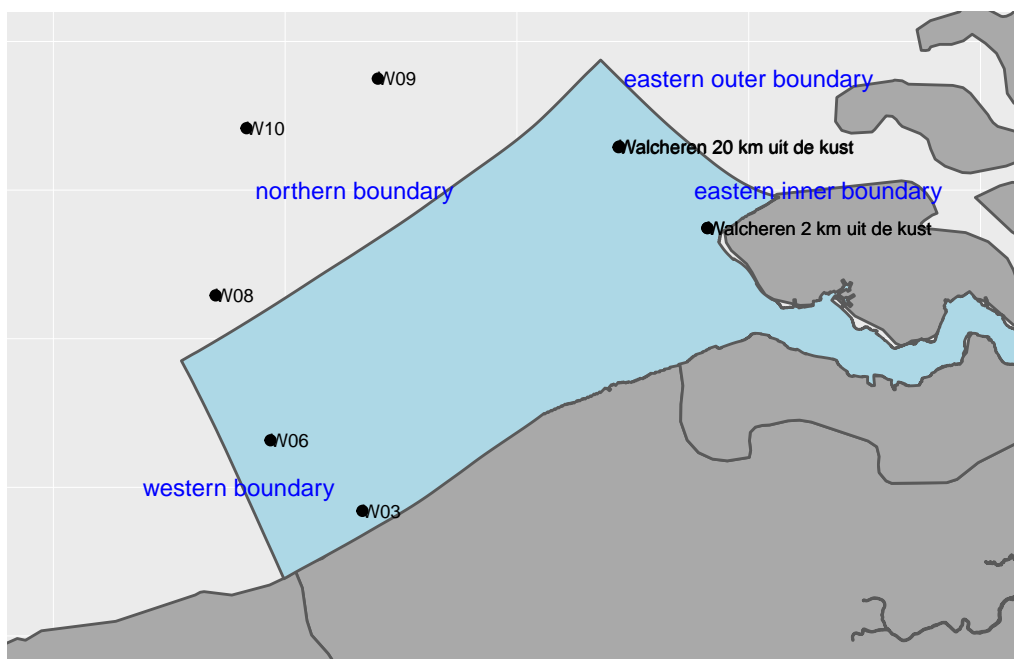


**Figure 3.5:** Seaward boundary of the model grid, with boundary names (blue) and measurement locations used to compose the water quality boundary conditions.

### 3.5 Boundary conditions

The boundary at the North Sea consist of a transversal part and a longitudinal part 3.5. The observations used for calculating boundary conditions are obtained from monitoring data close to the boundary.

Around the boundaries, there are several stations with relevant monitoring data. Close to the eastern boundary, the stations Walcheren 2 and Walcheren 20 had frequent observations of relevant substances. The observations of these two stations differed substantial from each other, which motivated the choice to split the eastern boundary in two parts, an inner part and an outer part. Walcheren 2 km uit de kust observations were used to construct the eastern inner boundary, and Walcheren 20 km uit de kust were used to construct all other boundaries. The other stations were not used in the boundary, because they contained less parameters, less observations, and their concentrations did not differ substantially from concentrations at Walcheren 20 km uit de kust. Concentrations were interpolated to obtain a boundary concentration at every time step.

The substances in the model were calculated from the observed concentrations according to:

modelled OXY = observed O<sub>2</sub> modelled Salinity = 0.5 modelled NH<sub>4</sub> = observed NH<sub>4</sub>  
 modelled NO<sub>3</sub> = observed NO<sub>3</sub> modelled PO<sub>4</sub> = observed PO<sub>4</sub> modelled Si = observed Si  
 modelled Opal = 0 modelled POC1 = measured POC modelled PON1 = observed POC \* 0.0714  
 modelled POP1 = observed POC \* 0.0085 modelled DOC = observed DOC modelled Diatoms  
 = observed chlfa x 0.5 x 40/1000 modelled Greenalgae = observed chlfa x 0.5 x 40/1000

The upstream boundary of the model exists of 6 freshwater sources (Schelde, Zenne, kleineNete, groteNete, Dijle, Dender) and 2 additional nutrient loads , (Bath, Terneuzen). In the hydro-

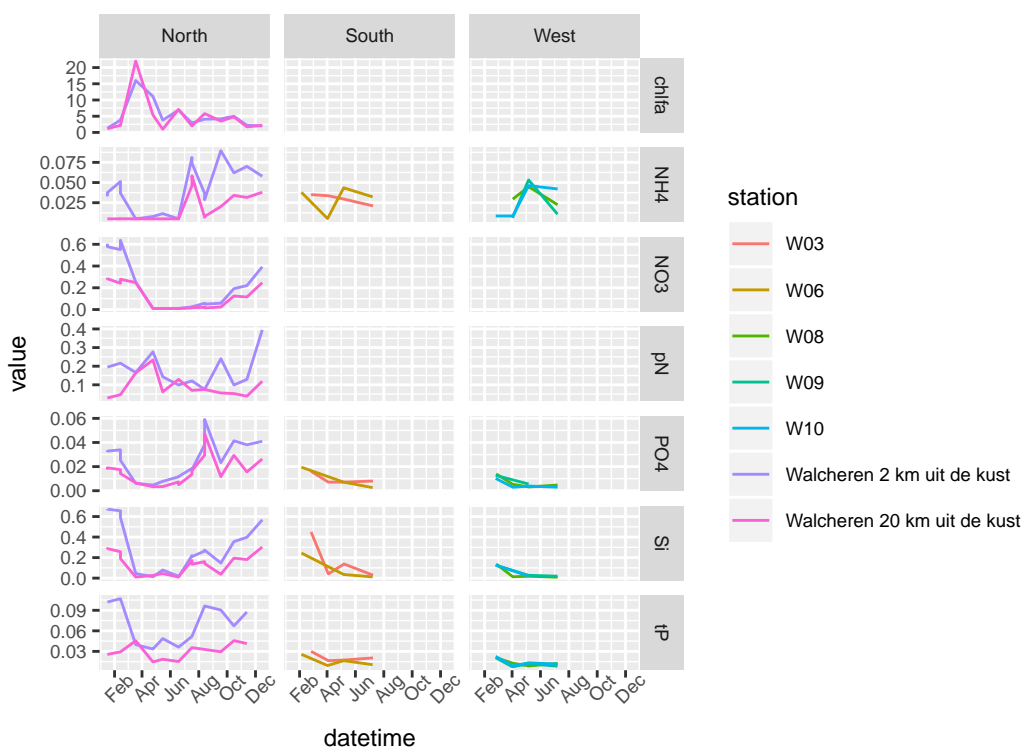


**Figure 3.6:** Concentrations of relevant substances at the model sea boundary.

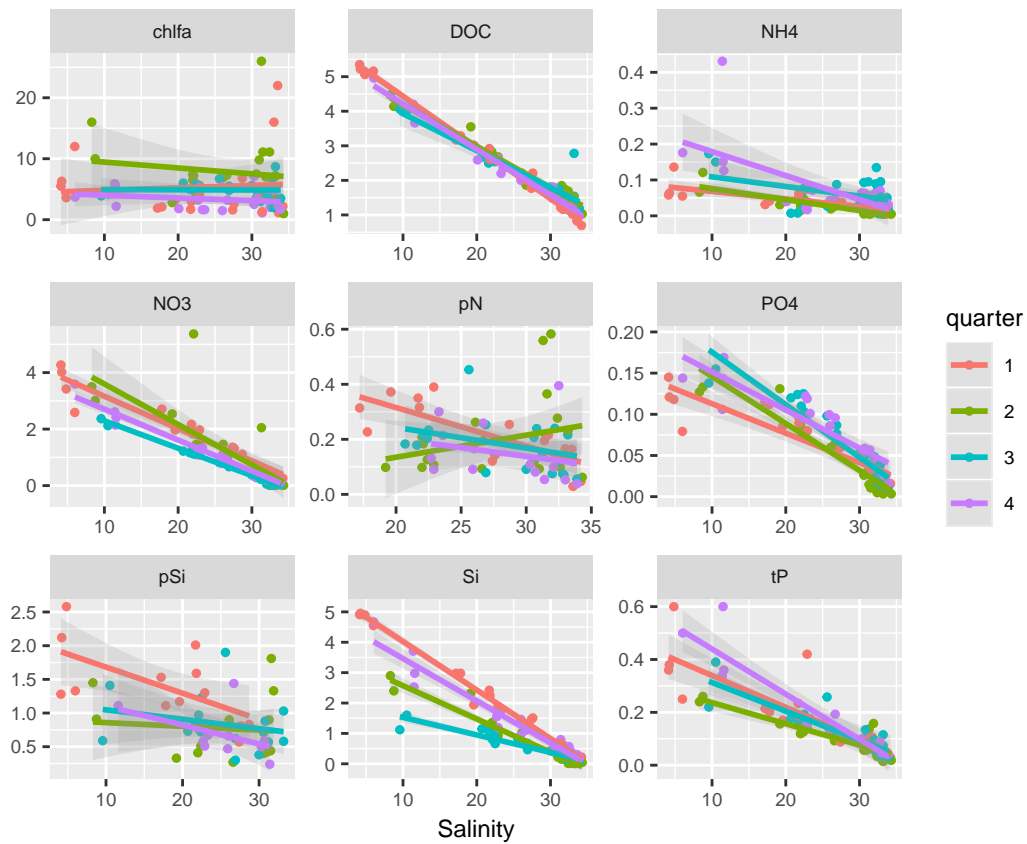
dynamic model, water flows have been implemented. The hydrodynamic flow was modelled with a time interval of 30 minutes. For performance reasons, this was aggregated to daily averaged flows for use in the water quality model.

In the upstream river part, nutrients are added by different point and diffuse sources. Rather than estimating all different sources, the total loads of substances in the freshwater part of the model were estimated from their correlation with salinity. Using this relationship, freshwater boundary concentrations were estimated by extrapolation to a salinity of 0 assuming a linear relationship (3.7). Estimations were made for each quarter of the year (Jan-Mar, Apr-Jun, Jul-Sep, Oct-Dec). Higher time resolution was not supported by the data. This method should be valid under the assumption that transport and mixing is more important than internal processes in the river. This assumption was met for the parameters chlorophyll-a, DOC, NH<sub>4</sub>, NO<sub>3</sub>, pN, pSi, Si, tP. The assumption did not appear to be valid for dissolved oxygen, which is in continuous exchange with the atmosphere and for POC.

From the above correlation, the concentrations of substances in the model were estimated. (table 3.1).

POC correlated poorly with salinity. Its mean concentration 1.5 mg C/l was therefore used for the freshwater boundary. For dissolved oxygen, a concentration of 10 mg/l was used in the freshwater boundary, assuming that concentrations will be in equilibrium with the atmosphere by the time the water reaches the Dutch part of the estuary. Other substances were transformed from these observed parameters in the following way.

modelled OXY = 10 mg O<sub>2</sub>/l  
 modelled Salinity = 0.5 PSU  
 modelled NH<sub>4</sub> = observed NH<sub>4</sub> mg N/l  
 modelled NO<sub>3</sub> = observed NO<sub>3</sub> mg N/l  
 modelled PO<sub>4</sub> = observed PO<sub>4</sub> mg P/l  
 modelled Si = observed Si mg Si/l  
 modelled Opal = observed pSi mg Si/l  
 modelled POC1 = 1.5 mg C/l

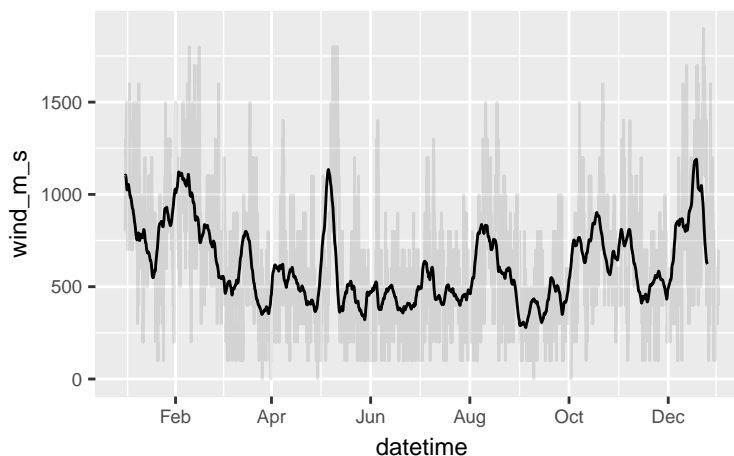


**Figure 3.7:** Correlations of dissolved substances with salinity per season in 2014. The freshwater boundary concentration was based on the extrapolation values of the substances to salinity = 0 promille for the different seasons.



**Table 3.1:** Estimated concentrations for upstream boundaries

time	chlfa	DOC	NH4	NO3	pN	PO4	pSi	Si	tP
01/01/14/00:00:00	4.4	5.9	0.089	5.3	0.600	0.15	2.10	5.6	0.46
01/04/14/00:00:00	10.0	5.4	0.110	6.0	-0.026	0.20	0.91	3.7	0.32
01/07/14/00:00:00	5.0	5.0	0.140	4.3	0.390	0.24	1.20	2.1	0.42
01/10/14/00:00:00	4.4	5.5	0.250	4.8	0.330	0.20	1.40	4.9	0.61

**Figure 3.8:** Wind speed at Vlissingen in m/s. hourly values (grey) weekly running means (black)

modelled PON1 = observed pN mg N/l modelled POP1 = observed tP - PO<sub>4</sub> mg P/l modelled DOC = observed DOC mg C/l modelled Diatoms = observed chlfa \* 50/1000 mg C/l modelled Greenalgae = 0

### 3.6 Meteo input

Meteo data were downloaded from the data repository of the Royal Dutch Meteorological Institute (<https://www.knmi.nl>) for the location Vlissingen, and used as a spatially uniform time series for the whole model grid.

Wind speed was applied as hourly values. In the water quality model, wind speed is only used to regulate the exchange of dissolved oxygen with the atmosphere.

Solar radiation was applied as a spatially uniform time series (function). Hourly radiation values for the KNMI station “Vlissingen” was used for the whole grid. Using hourly values for radiation is necessary for calculating realistic daily variation of dissolved oxygen concentrations in the water. Solar irradiance is converted to underwater irradiances by the model taking into account the backscatter at the water surface layer and the extinction due to DOC, SPM, POC and Chlfa, as well as a background extinction.

### 3.7 Substances and processes

The following substances are modelled:

The most important processes are explained below For a detailed description of all processes, we refer to the D-Water Quality User Manual (Deltares (2016)).

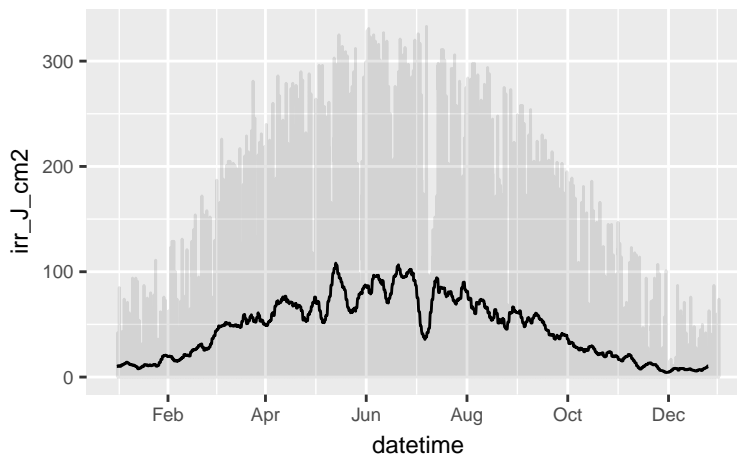


**Figure 3.9:** Irradiation at Vlissingen in J/cm2. Hourly values (grey) weekly running means (black)

### 3.8 Primary production by phytoplankton

In a previous version of the model Stolte and van Oorschot (2012), the phytoplankton module “BLOOM” was used to model different species of phytoplankton. For the current model, a simpler model, DYNAMO, was used. The reason for that was twofold.

1. The strength of BLOOM is that it computes many different phytoplankton species with well tested characteristics. However, BLOOM calculates states every 24 hours, and implicitly assumes more or less constant conditions for a given bulk of water over that period. In the Schelde, water travels over deeper and shallower part twice a day. This makes BLOOM less suitable. DYNAMO calculates states with every timestep of the water quality model, which is typically 10 minutes.
2. The model results of oxygen concentration will be compared with the continuous oxygen measurements in the Schelde in a parallel project. Therefore, oxygen needs to be calculated with short time steps (10-15 minutes). This can not be done using BLOOM because it only calculates primary production-related states every 24 hour.

Two DYNAMO phytoplankton species are included in the model: Diatoms and Greens (non-diatoms). The major difference between the two is that diatoms need silica for their growth. Diatoms have higher affinity for light and a slightly higher maximum specific growth rate, which makes them better competitors than greens in spring when still ample silicate is available.

DYNAMO algae have a direct growth response to environmental nutrient concentrations (nitrate, ammonium, phosphate, silicate) and light availability, using a hyperbolic functional response for nutrients (Monod (1949)) and a threshold response for light as in e.g. Slagstad (1982).

Overall equation of phytoplankton processes:

$$dPhyt/dt = \text{loads} + \text{transport} - \text{settling} + \text{resuspension} + \text{grossPrimaryProd} - \text{respiration} - \text{mortality}$$

$$R_{gpi} = f_{nut_i} * f_{lt_i} * k_{gpi} * Calg_i$$

with

**Table 3.2:** List of substances (state variables) used in the model.

code	description
Continuity	Continuity
OXY	oxygen concentration
Salinity	salinity in psu
NH4	ammonium concentration in mgN/l
NO3	nitrate concentration in mgN/l
PO4	dissolved reactive phosphate concentration in mgP/l
AAP	adsorbed anorganic phosphate concentration in mgP/l
Si	dissolved silicate concentration in mgSi/l
Opal	particulate silicate concentration in mgSi/l
POC1	dead particulate organic carbon concentration in mgC/l
PON1	dead particulate organic nitrogen concentration in mgN/l
POP1	dead particulate organic phosphorus concentration in mgP/l
DOC	dissolved organic carbon concentration in mgC/l
Diat	diatom biomass concentration in mgC/l
Green	non-diatom biomass concentration in mgC/l
DetCS1	dead particulate organic carbon concentration in the sediment in mgC/l
DetNS1	dead particulate organic nitrogen concentration in the sediment in mgN/l
DetPS1	dead particulate organic phosphorus concentration in the sediment in mgP/l
DetSiS1	dead particulate organic silicate concentration in the sediment in mgSi/l

$C_{alg}$ : algal biomass concentration in  $gCm^{-3}$

$f_{lt}$ : light limitation factor [-]

$f_{nut}$ : nutrient limitation factor according to Monod [-]

$k_{gp}$ : potential gross primary production rate in  $d^{-1}$

$R_{gp}$ : gross primary production rate in  $gCm^{-3}d^{-1}$

$i$ : index for species group (Diat or Green)

Nutrient limitation is calculated using Monod kinetics,  $f_{nut} = nut / (K_{m,nut} + nut)$  with  $nut$  is the nutrient concentration, and  $K_{m,nut}$  is the half-saturation constant for growth for this particular nutrient, considering all other nutrients are in excess. In case multiple nutrients are limiting, the most limiting nutrient determines the growth rate.

Light limitation is a combination of a day length factor and a radiation limiting factor that saturates for day length and light intensities larger than the optimal day length and a saturating light intensity. Light inhibition is not modelled.

The depth averaged light intensity is derived according to Lambert-Beer's Law for light attenuation:

$$I_z = I_{top} * e^{-ec*z}$$

with:

$ec$  = extinction coefficient of visible light in  $m^{-1}$

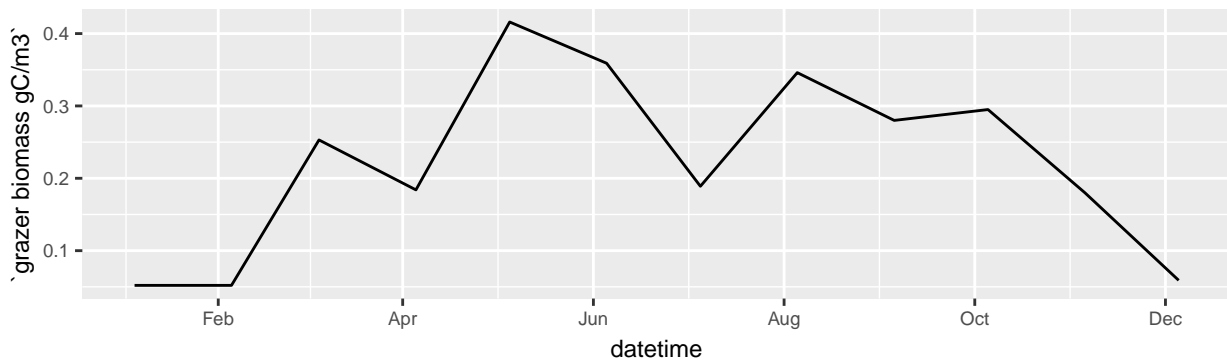


**Figure 3.10:** Forced potential biomass of zooplankton in the model, based on measurements

$I_{top}$  = light intensity at the top of a water layer in  $Wm^{-2}$

$z$  = water depth in  $m$

The extinction coefficient is the sum of contributions of the background (water plus not modelled substances), live algae biomass, particulate and dissolved detritus and inorganic suspended matter. These contributions follow from the multiplication of concentrations and specific extinction coefficients.

### 3.9 Phytobenthos

Primary production by phytobenthos is not yet included in the model. The algal growth module that is used in this study (DYNAMO) is suitable, but validation data are missing. Therefore, this has not been prioritized yet.

### 3.10 Grazing by zooplankton

Zooplankton grazing has been added to the model as a spatially homogeneous time series of potential grazing pressure (semi-forcing function). The process that is used for this (CONSBL) calculates grazing on algae based on grazer preference, a potential (maximum) concentration of zooplankton grazers, while temperature is a regulating environmental factor.

Pelagic grazing was forced using a grazer biomass based on measurements from the previous model version (2006).

### 3.11 Grazing by macrozoobenthos

Grazing by macrozoobenthos on phytoplankton is not yet included in the model. There is a model description available in the used software, which can be readily applied. However, some choices will have to be made, such as parameterization (depending on species or group of macrobenthos) and initialization

## 4 Results

Before any calibration, the model was run with default values for constants, except the rate for phosphate adsorption and desorption to suspended inorganic material. This rate was lowered as compared to default values to avoid occurrence of negative phosphate concentrations in parts of the river with very high concentrations of suspended sediment and high concentrations of phosphate. Since suspended sediment is forced upon the model, its concentration may change quickly as compared to other variables. Dissolved phosphate then adsorbs to the newly established suspended sediment concentration at rates that are sometimes too high for the time step, resulting in negative concentrations of dissolved phosphate. Lowering the rate constant effectively avoided these negative concentrations.

### 4.1 Salinity and total nutrients

The model was run for 1 year to spin up. The final situation of that year was used as a starting point for the runs that are presented here.

Salinity is recalculated by the water quality model. Any deterioration of the calculated salinity as compared to the hydrodynamic model might indicate an effect of e.g. the horizontal aggregation, or a too large time step.

The seasonal variation of salinity is well-captured by the model. On average, the salinity is underestimated as compared to observations at these locations. However, the underestimation is comparable to the results of the hydrodynamic model. Moreover, although the running average is overestimated, the model result at exactly the point of monitoring is not necessarily underestimated in the same way due to the high daily variation (grey lines in plot).

The average concentration of total nutrient concentrations in the Westerschelde was estimated correctly. This is consistent with the good fit of salinity, since transport is more important than processes for the variation of total nutrients. The process that could disturb the good relationship between salinity and total nitrogen concentration in the estuary is denitrification. For phosphorus, adsorption/desorption processes could disturb the correlation of total phosphorus with salinity. The variation due to uptake by algae in spring and summer was delayed, which is consistent with the underestimated biomass of phytoplankton at e.g. Schaar van Ouden Doel.

The target diagram summarizes the comparison of model and observations at the exact moment of monitoring. Vertically, the average normalized bias is plotted, and horizontally, the normalized unbiased RMSD. On average, salinity is underestimated, least in Walcheren, and most in Hansweert. Total nitrogen and phosphorus are also slightly underestimated, to a lesser extent or even overestimated at Hansweert, which is consistent with the salinity deviation. At most stations, the model does not reproduce all variability in the monitoring data.

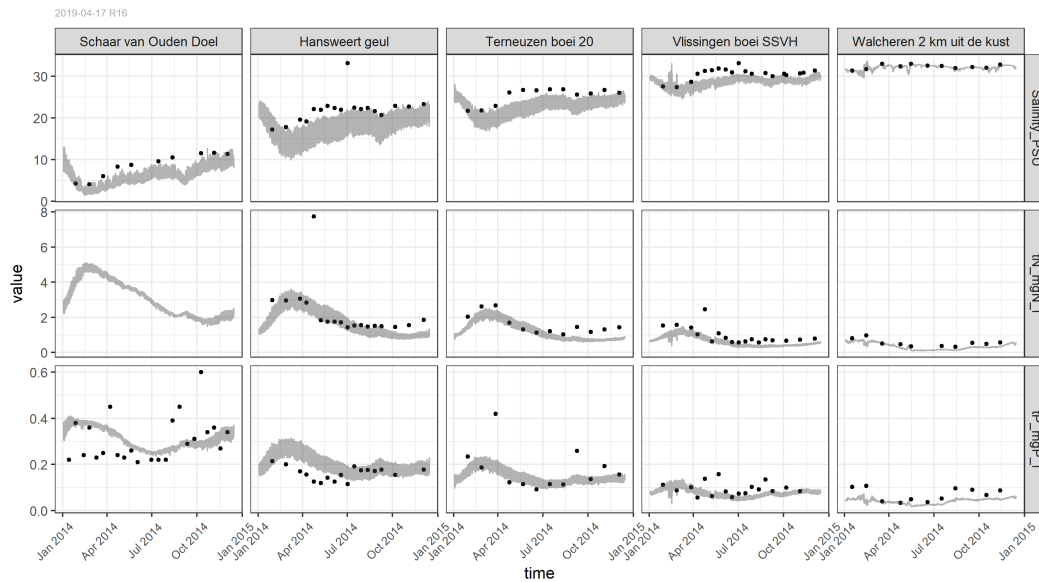


**Figure 4.1:** Model-data comparison for salinity and total nutrient concentration at the MWTL monitoring stations for the uncalibrated model

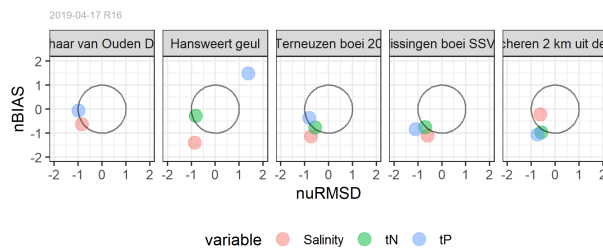


**Figure 4.2:** Target diagram for model performance: salinity, total nitrogen and total phosphorus

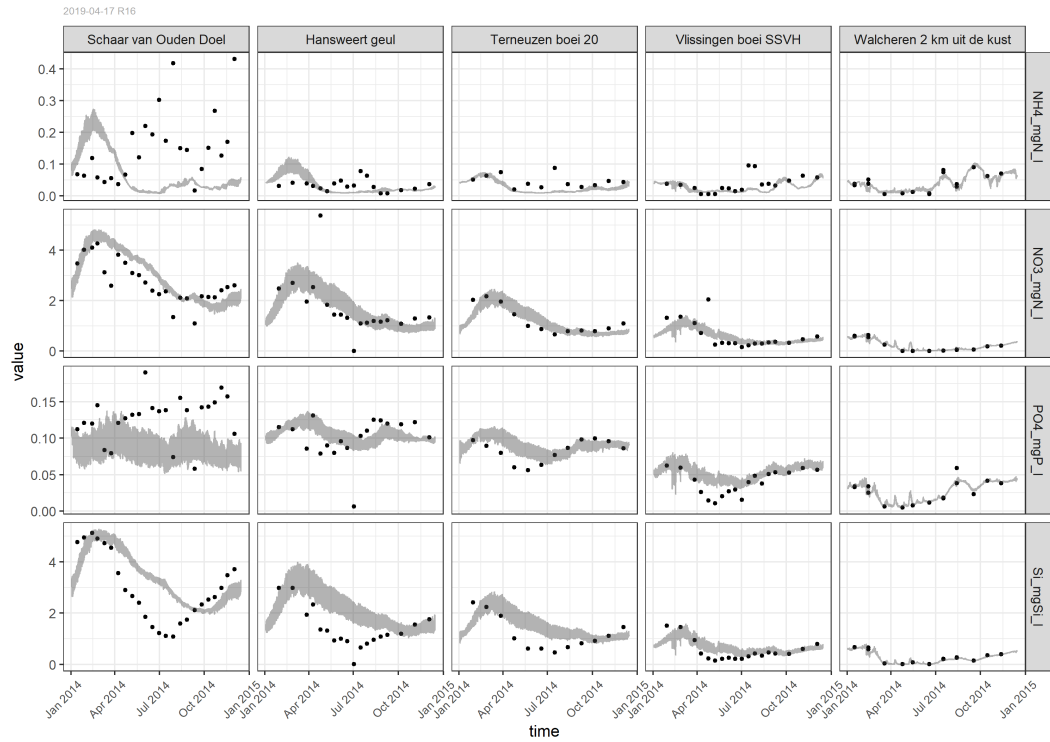


**Figure 4.3:** Model-data comparison for inorganic nutrients at the MWTL monitoring stations for the uncalibrated model

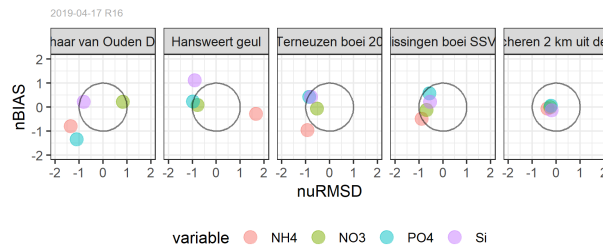


**Figure 4.4:** Target model performance diagram for inorganic nutrients at the MWTL monitoring stations for the uncalibrated model

## 4.2 Inorganic nutrients

Nitrate concentrations are reproduced well by the model. Only at Schaar van Ouden Doel, the decrease of nitrate during spring/summer is underestimated, probably due to the underestimation of phytoplankton biomass at that station.

The observations show an increase in the concentrations of inorganic phosphate and ammonium in late summer, probably due to remineralization and/or redelivery from the sediment. This is not reproduced well by the model. Average concentrations are reproduced well, indicating that the upstream and North Sea boundaries have been estimated well. Target diagrams show that especially NH<sub>4</sub> and PO<sub>4</sub> variability is underestimated at Schaar van Ouden Doel. On average, the concentrations are well described by the model.

## 4.3 Suspended sediments (SPM), light extinction coefficient (E), dissolved organic matter (DOC) and chlorophyll-a (Chlfa)

SPM and DOC are the two components that have largest effect on light extinction, thereby potentially also on phytoplankton growth.

Without calibration, phytoplankton biomass expressed as chlorophyll a is underestimated by the model at the relative upstream stations Schaar van Ouden Doel, Hansweert and Terneuzen. At the mouth of the Westerschelde (Vlissingen) chlorophyll a is at average calculated correctly.

Close to the model boundary (Walcheren), chlorophyll is overestimated. The reason for this is that the boundary conditions are formulated based on phytoplankton carbon. The chlfa/C ratio of the algae used is applied as for light-limited phytoplankton (as occurring in the Westerschelde), which is higher than the naturally occurring phytoplankton in the coastal waters. To estimate chlfa/C well across the whole model grid, the algal module should have variable chlfa/C ratio. The module DYNAMO that is used in this version of the model does not have this possibility see section @dynamo.

MWTL sampling occurs at one hour before high tide. The underestimated chlorophyll can be partly explained by an overestimated total extinction coefficient at Schaar van Ouden Doel in the first months of the year. Especially at Hansweert and Terneuzen, the extinction coefficient is underestimated in the first few months, as compared to the MWTL observations. can at these stations be partly explained by low suspended sediment concentration, especially in the first months of the year.

In general, modelled suspended sediment concentrations are highly variable over the tidal cycle. The comparison with MWTL biweekly measurements is therefore complicated. MWTL samples are taken one hour before high tide, which would normally not be associated with the highest SPM concentrations.

DOC is predicted well, and the overestimation at some stations is consistent with the underestimation of salinity.

The underestimated chlorophyll can be explained by:

- underestimated chlfa/C ratio
- underestimated growth due to overestimated extinction in first few months of the year
- underestimated physiological response of phytoplankton at low light
- underestimated production upstream



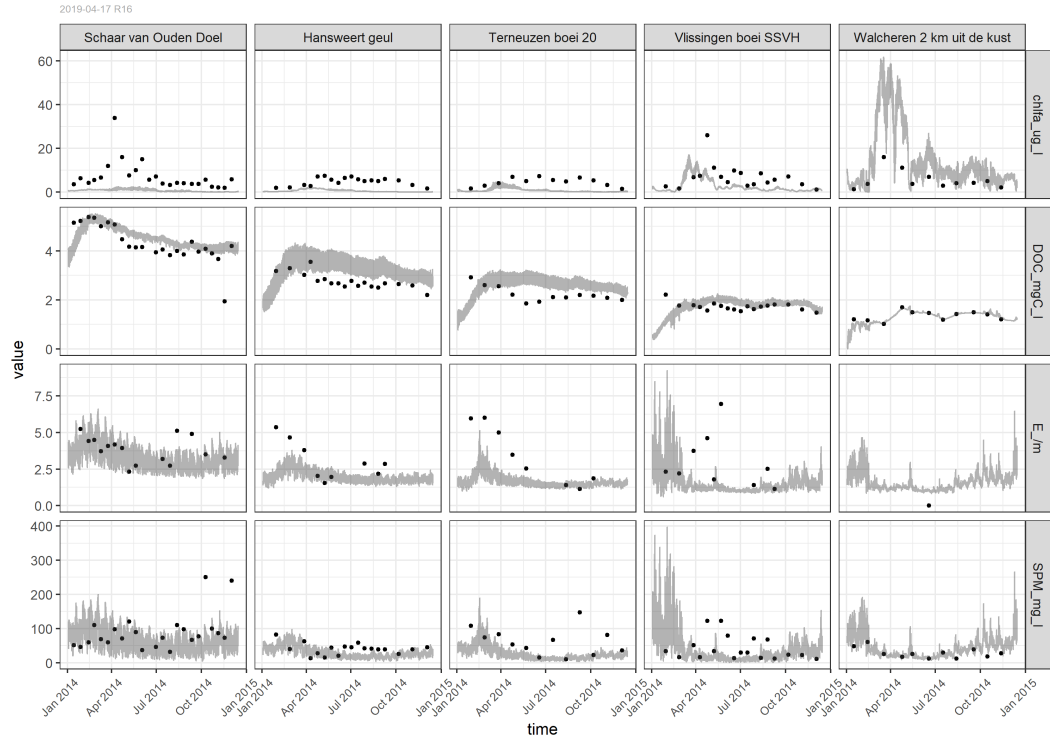


**Figure 4.5:** Model-data comparison for SPM, E, DOC, and Chlfa at the MWTL monitoring stations for the uncalibrated model

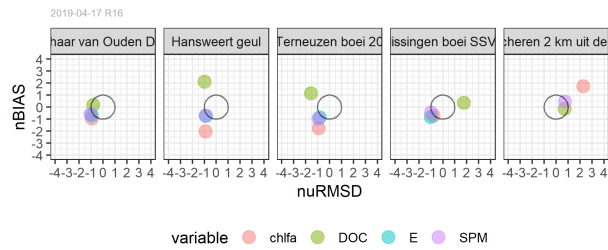


**Figure 4.6:** Target model performance diagram for SPM, E, DOC, and Chlfa at the MWTL monitoring stations for the uncalibrated model

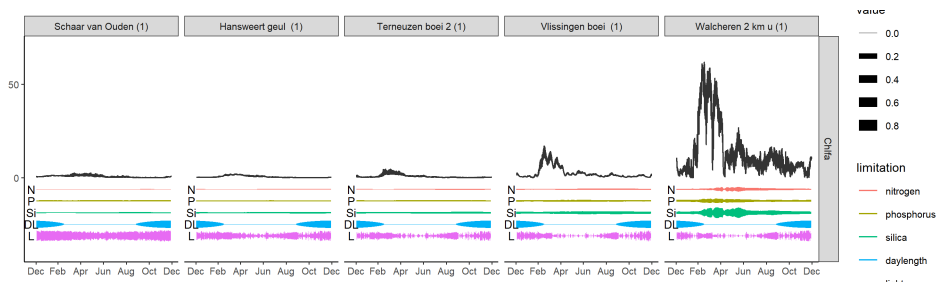


**Figure 4.7:** Strength of limiting factor for diatom growth in the top layer as compared to chlorophyll a biomass before calibration. The thickness of the colored bands is indicative for the relative limitation by that factor

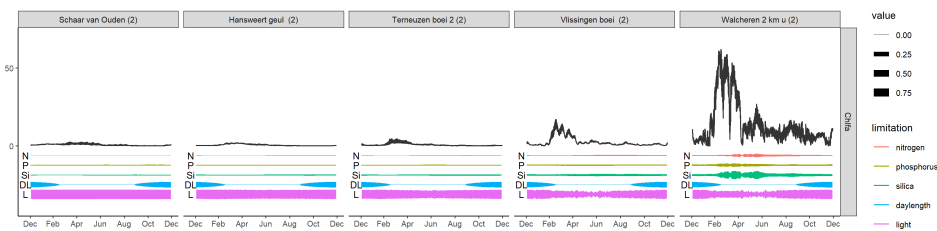


**Figure 4.8:** Limiting factors in the second layer

#### 4.4 Limiting factors for phytoplankton production and biomass

limiting factor for primary production is light in virtually the whole Westerschelde. Only in the coastal station, silicate limitation exceeds light limitation, but of course only for diatoms. Phytoplankton biomass is further limited by the loss factors, which are sedimentation, (auto)mortality and grazing. Light limitation in the second layer is already much stronger than in the top layer, due to the high extinction of light by suspended sediments and DOC.

#### 4.5 Calibration and validation rationale

A general issue in calibration of phytoplankton growth in any model is that most measurements are available of phytoplankton biomass concentration, either as cell counts or as measured concentrations of particulate chlorophyll-a. Since the phytoplankton biomass as chlorophyll-a at a given moment depends on growth, mortality, grazing, sedimentation, and residence time, issues related to calibration of phytoplankton or chlorophyll a are numerous:

- Growth and loss (mortality, grazing, sedimentation) rates are often in similar order of magnitude. The resulting biomass is therefore quite sensitive to small variation in either growth or loss factors. Only in clear spring bloom situations, growth of phytoplankton is temporarily decoupled from loss factors. Due to the poor light conditions in the Schelde, this is not very common in this estuary.
- Chlorophyll a concentration is a very sensitive indicator for phytoplankton, but not very accurate. Chlorophyll a to carbon ratios vary easily a factor of 4 or more driven mostly by light and nitrogen availability (ref). Moreover, measured chlorophyll a could be due to resuspended benthic microalgae, especially in estuaries with tidal flats and high flow velocities.

#### 4.6 Calibration of DOC light extinction coefficient

In the non-calibrated model, algal biomass is highly underestimated in the Westerschelde stations upstream of Vlissingen. Light is the limiting factor. Concentrations of the main contributing substances (*SPM* and *DOC*) are estimated reasonably well. There are then two possible ways to correct for the low biomass in the model.

- Adapt the algal growth parameters so that they will grow better at low light
- Adapt the light extinction coefficient in the water so that more light is available for the algae.

Although light extinction coefficients were not overestimated in the Westerschelde as compared to the measurements (figure) the gradient of the light extinction through the estuary is not reproduced correctly. Observations show a maximum extinction coefficient downstream of Schaar van Ouden Doel. Contrary, the model shows on average maximum extinction coefficients at Schaar van Ouden Doel, especially during the growth season.

Initial light extinction coefficients were calculated using observed SPM, DOC and chlorophyll-a concentrations, as a function of measured extinction coefficients *E* according to equation

$$E_{SPM,DOC} = a + b * [SPM] + c * [DOC] + d * [Chlfa]$$

with coefficients as in table xx.

The dependency of *E* with DOC shows highest uncertainty in the calculation of *E*. Therefore, coefficient *c* was chosen as a calibration parameter. Also, DOC is inversely proportional to salinity, and its extinction will have a larger effect at Schaar van Ouden Doel, where phytoplankton is underestimated.

The result of lowering the extinction coefficient for DOC was that in the intermediate stations, Hansweert and Terneuzen, chlorophyll-a concentrations matched better with the observations. At Schaar van Ouden Doel, phytoplankton biomass, expressed as chlorophyll, also increased, but was still underestimated.

#### 4.7 Calibration by change of phytoplankton growth parameters

Phytoplankton growth in the estuary is limited by light. Low production and biomass at station Schaar could be due to a relatively low response of phytoplankton. There are roughly three ways to increase the net growth of phytoplankton in such a light limited system

1. Increase the light affinity - This will increase the growth response of phytoplankton during light limitation. Upon testing indeed phytoplankton biomass at Schaar van Ouden Doel increased generally, and especially in spring, which fitted much better to the observations. However, at stations downstream of Schaar van Ouden Doel, phytoplankton biomass was highly overestimated during the spring bloom, which was not seen in the observations.
2. Increase the maximum growth rate - this was not tested. Increasing this parameter will lead to unnaturally high maximum growth rates. An increase would result in a quick increase of phytoplankton during favorable conditions. This can be applied when the variability in phytoplankton concentration is highly underestimated.
3. Reduce the mortality rate - Specific mortality rate default value was relatively high (0.35). Since also grazing is incorporated as a separate process, mortality could be reduced. Expected result is that biomass will increase, and because of the longer life of the phytoplankton, biomass will spread more over time and space. A generally higher biomass of time and space will be the expected result. Based on the previous calibration run, this adaptation was chosen as a next step.

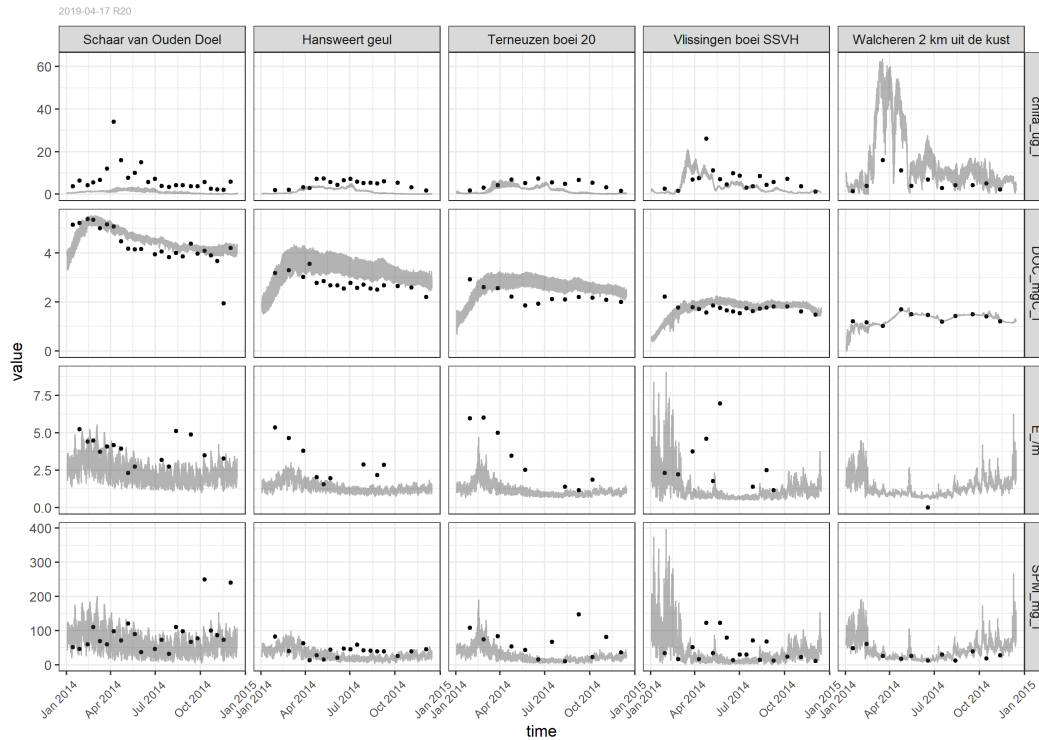


**Figure 4.9:** Model-data comparison for SPM, E, DOC, and Chlfa at the MWTL monitoring stations after lowering the specific extinction coefficient for DOC

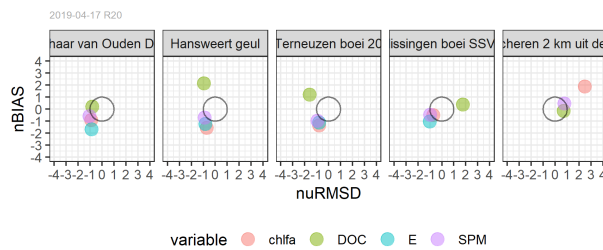


**Figure 4.10:** Target diagram for SPM, E, DOC, and Chlfa at the MWTL monitoring stations after lowering the specific extinction coefficient for DOC

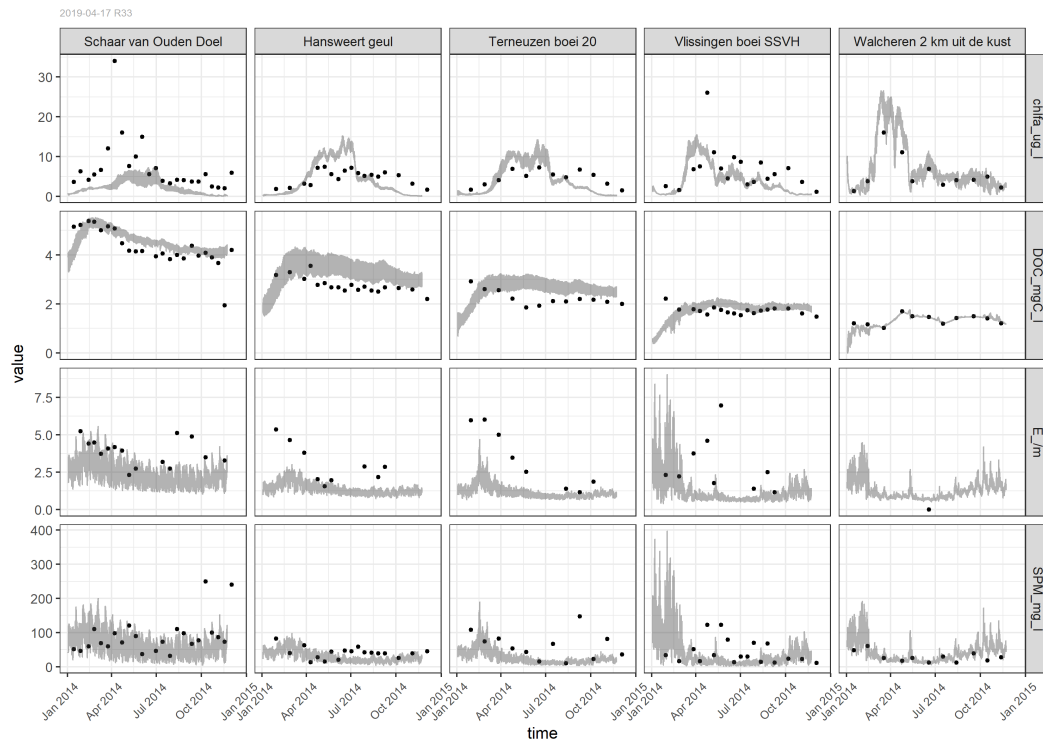


**Figure 4.11:** Modelled (line) and observed (dots) SPM, Extinction coefficient E, DOC, and Chlorophyll a for the model calibration run with decreased extinction coefficient for DOC and decreased mortality rate for diatoms and non-diatoms.

The result of the 3rd adaptation is seen in the figure below. Modelled biomass at Hansweert, Terneuzen, and Vlissingen fitted much better to the observations. At Schaar van Ouden Doel, Chlorophyll was still underestimated. However, this is consistent with the very low C:Chlfa ratio found in the phytoplankton observations at that location.

The modelled Chlorophyll a concentration was much improved as compared to the previous run. Decrease of mortality rates increased the biomass, and thus chlorophyll-a concentration over the whole growth season. Still, the shape of the spring increase of chlorophyll at e.g. Vlissingen is very sharp, which in the model is explained by the steep decrease of SPM and subsequent E. In the observations, these sudden changes are more modest, absent, or even reversed. At point, the variation in E/SPM at some sampling occasions is not fully understood.

Chlorophyll-a at Schaar van Ouden Doel is still underestimated. This is not necessarily a

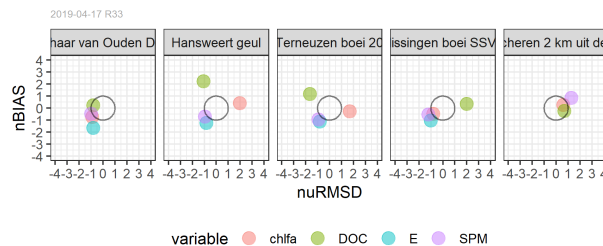


**Figure 4.12:** Target diagrams for the model calibration run with decreased extinction coefficient for DOC and decreased mortality rates.

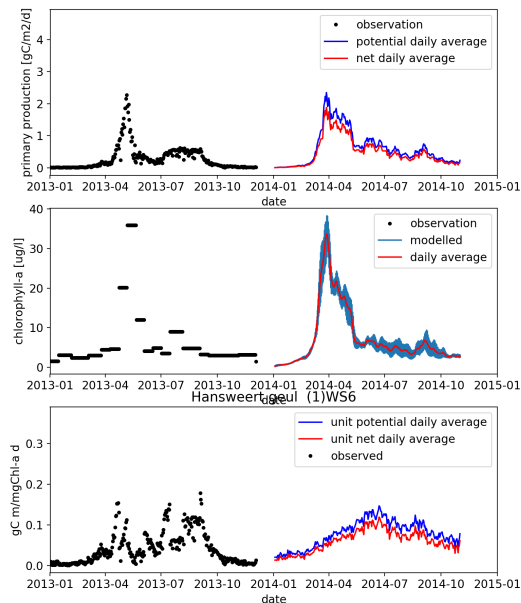


**Figure 4.13:** Observed and modelled depth integrated primary production (top), chlorophyll-a during production measurements (middle), and specific primary production as  $gC/mgChlfa/day$  (bottom) at station Hansweert Geul. Observations from 2014 were not available for stations in the Westerschelde. Data were kindly provided by Dr. Jacco Kromkamp, Royal Netherlands Institute for Sea Research (NIOZ).

problem, because phytoplankton at this station displays a very low carbon to chlorophyll-a ratio. The modelled phytoplankton have a much higher carbon to chlorophyll-a to carbon ratio.

The variability of chlorophyll-a is still overestimated at stations Hansweert geul and Terneuzen boei. Possibly, mortality rates may be reduced even more. However, upon trying, this resulted in even higher variability due to too fast growth. Further calibration should be directed towards balancing the ratio between growth and loss factors of the phytoplankton in such a way that enough biomass is produced, but variability does not increase too much.

#### 4.8 Comparison of modelled and measured primary production

Primary production was measured in the Schelde, but to a lesser extent in the Westerschelde in the scope of the MONEOS monitoring projects (<http://www.scheldemonitor.be/nl/monitoringsprogramma-moneos>). For the year 2014, there are no observations in the Westerschelde. Comparing nearby station Hansweert model results with observations from the previous year, the modelled specific primary production ( $mgC/\mu gChlfa$ ) compared reasonable well with the observed values throughout the season.

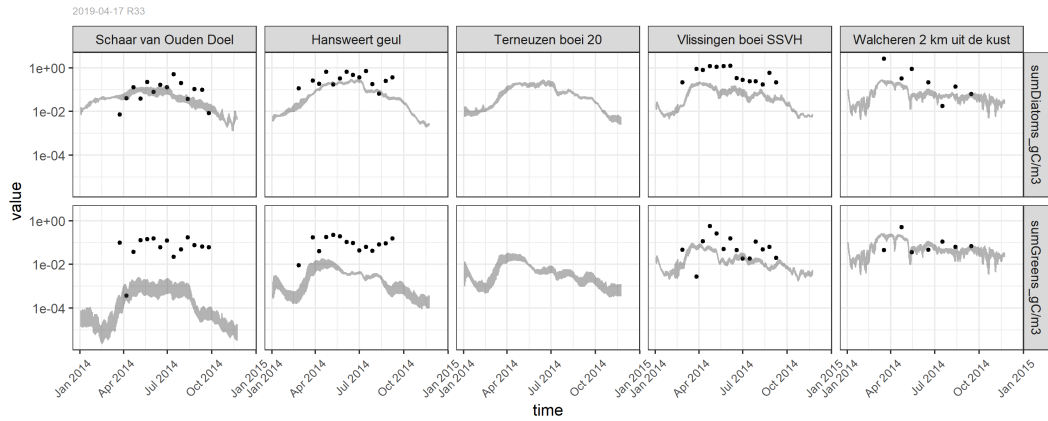


**Figure 4.14:** Model - observation comparison for phytoplankton biomass in carbon for the model calibration with 1. decreased extinction coefficient for DOC, and 2. decreased mortality of the diatoms and non-diatoms.

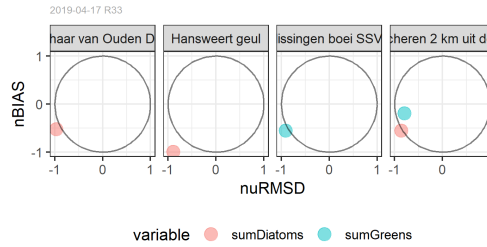


**Figure 4.15:** Target diagrams for phytoplankton biomass in carbon for the model calibration with 1. decreased extinction coefficient for DOC, and 2. decreased mortality of the diatoms and non-diatoms.

#### 4.9 Phytoplankton groups and biomass

The biomass of phytoplankton expressed as carbon was reasonable. Diatom biomass was estimated well at Schaar van Ouden Doel and Hansweert geul, and underestimated, but reasonable at the other stations. The reason for the underestimation is not clear. At Vlissingen, silicate is not limited (see section @limitations) .

Non-diatoms (Greens in the model) were estimated well at the other stations, and underestimated at Schaar van Ouden Doel and Hansweert.

#### 4.10 Dissolved oxygen

The seasonal dynamics of oxygen concentration was modelled correctly. However, the average concentration was overestimated during the whole year, especially at Schaar van Ouden Doel (figure 4.17).

The explanation for this must be that the saturation concentration for oxygen is not estimated correctly. This saturation concentration is determined by salinity and temperature. Salinity is underestimated by the model (4.1). Since freshwater can contain more dissolved oxygen than seawater, modelled oxygen would be overestimated.

Modelled temperature is in general very well estimated, but slightly underestimated at Schaar van Ouden Doel. This would also cause an overestimation of dissolved oxygen concentration. Temperature is a forcing function based on the temperature at Terneuzen Boei 20 station. For a better temperature estimation, a spatially explicit definition will have to be used.

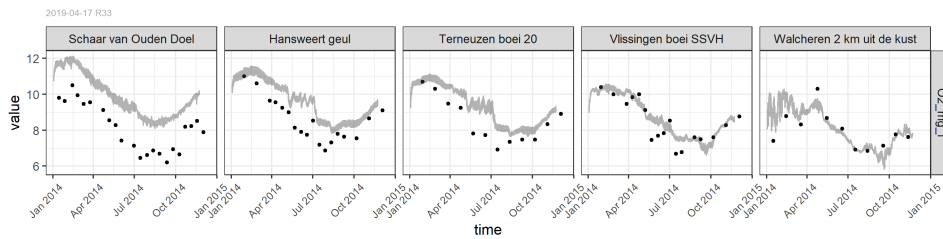


**Figure 4.16:** Modelled (line) and observed (dots) dissolved oxygen for the model calibration with 1. decreased extinction coefficient for DOC, and 2. decreased mortality of the diatoms and non-diatoms.

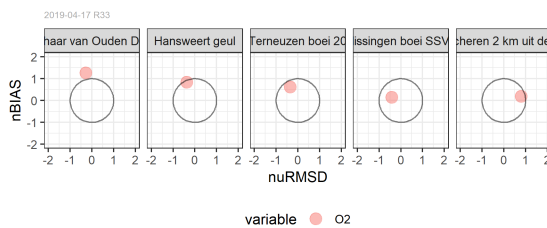


**Figure 4.17:** Target diagrams of model-observation comparison of dissolved oxygen for run 33.

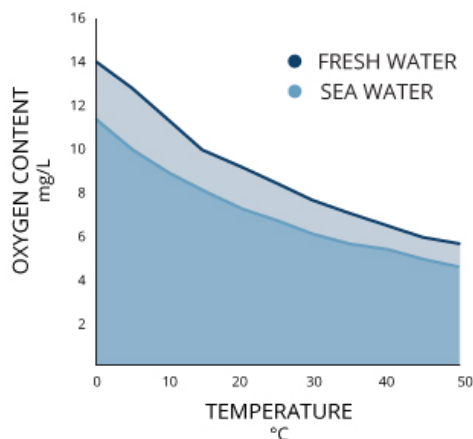


**Figure 4.18:** Saturation of dissolved oxygen dependent on salinity and temperature. From: Fondriest Environmental, Inc. "Dissolved Oxygen." Fundamentals of Environmental Measurements. 19 Nov. 2013. [weblink](<https://www.fondriest.com/environmental-measurements/parameters/water-quality/dissolved-oxygen/>)

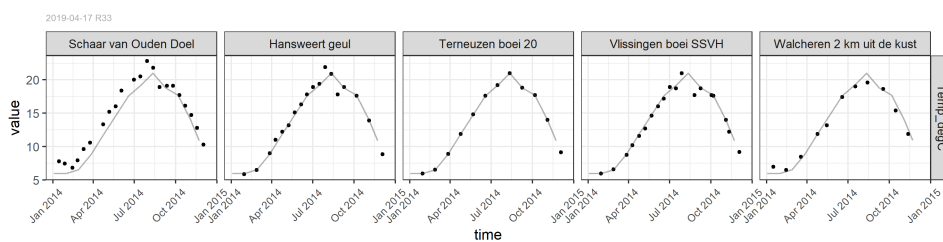


**Figure 4.19:** Modelled (line) and observed (dots) temperature for the model calibration with 1. decreased extinction coefficient for DOC, and 2. decreased mortality of the diatoms and non-diatoms.



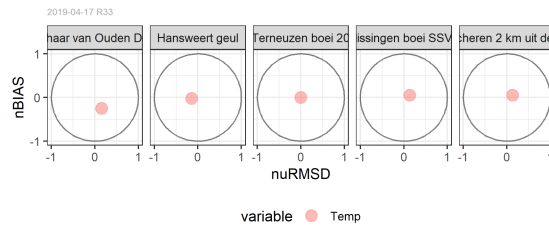


**Figure 4.20:** Target diagrams of model-observation comparison of dissolved oxygen for run 33.

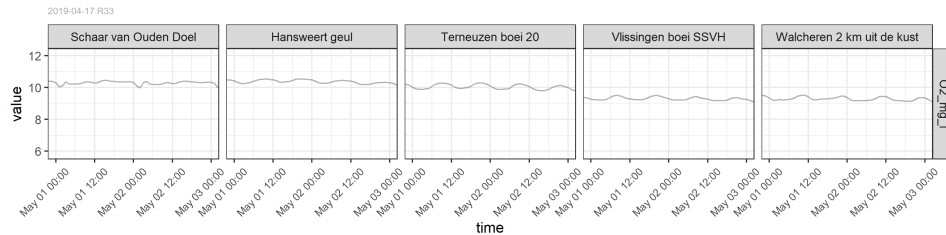


**Figure 4.21:** Modelled (line) diurnal patterns (2 days in beginning of May) of dissolved oxygen for the model calibration with 1. decreased extinction coefficient for DOC, and 2. decreased mortality of the diatoms and non-diatoms.

The diurnal variation of dissolved oxygen, which was one of the target values, is shown in figure (fig:O2Diurnal). Very clearly, there is a tidal (twice a day) cycle at some stations, e.g. Vlissingen, and additional signals which are caused by other processes such as production, consumption, reaeration. These results will later be used to be compared to continuous measurements. The variation over the day, rather than the absolute concentration is important for this comparison.

#### 4.11 Comparison with remote sensing data

A comparison between remote sensing information was made where possible. New algorithms for atmospheric correction and calculation of suspended matter were tested during a parallel project (Verhoog (2018)). In general, remote sensing data compared well to observations. In fact, the sediment model results at some locations (see for Vlissingen 4.22) compared better to the remote sensing derived SPM, than to the in situ observations.

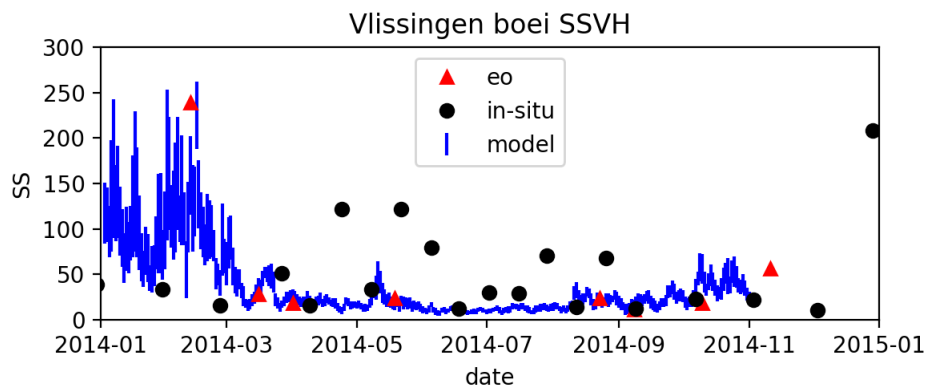


**Figure 4.22:** Comparison of SPM between model, in situ data and remote sensing derived information.



## 5 Conclusions

The update model of water quality and primary production for the Schelde has been set up, calibrated to fit phytoplankton biomass and production, and validated. The calibrated model produces consistent results and reproduces averages as well as variability of most substances and chlorophyll-a well for the Westerschelde area. However, the observations frequency of nutrients and phytoplankton (once every two weeks) is low relative to the modelled dynamics, hampering a fair comparison between model and observations. Calibration steps involved:

1. a reduction of the extinction coefficient of DOC, motivated by the high uncertainty in the initial estimation of this parameters.
2. a reduction of the mortality for diatoms and non-diatoms. This was motivated by the relative high value of this constant, given that phytoplankton grazing by zooplankton is included in the model.

Phytoplankton biomass in terms of carbon is still a bit underestimated, but the production and especially the chlorophyll-specific production was estimated well. The model shows consistent results and reacts as expected to changes in phytoplankton growth and mortality parameters, and physical parameters as SPM, DOC and the light extinction which is dominated by these two substances.

The spatial variation of nutrients and phytoplankton biomass was estimated well in the Westerschelde. In the river part, no validation was done at this stage.

We conclude that the model in its current form is suitable to predict changes in primary production as a result of changes in the regulating parameters.

### 5.1 Performance of the model in relation to the target variables

The model reproduces chlorophyll-a and phytoplankton biomass well. The target variable primary production was estimated well, based on measurements of a previous year. There are no data to validate the primary production rates directly, but given the above, there is considerable trust in the performance of the model to predict primary production by phytoplankton and its variation over the year

The target variable dissolved oxygen variation over the diurnal light/dark cycle was reproduced as expected. At this moment, no validation with high-frequency data could be done because data were not yet available. However, this validation will be subject to a more research-oriented project in the near future.

The current model describes transport of water and substances (salinity, total nutrients) well, showing realistic gradients in the Schelde estuary. Also, suspended solids gradients are in general realistic and conform observations. In detail, not all variability in suspended sediment is captured by the model.

In general, the model responds well to variability in environmental variables (temperature, light) during the growth season of 2014. Without calibration, phytoplankton biomass is underestimated at the station Schaar van Ouden Doel, which is in the upstream part of the Westerschelde. After calibration, which improved the biomass at Schaar van Ouden Doel greatly, biomass of phytoplankton during the spring bloom was overestimated in the middle and downstream part of the Westerschelde.

## 5.2 Uncertainties

Uncertainties are introduced in the final model results as a result of uncertainties in:

- Model input
  - Hydrodynamics - The salinity patterns predicted by the model fit in general well with the observations. However, in the Westerschelde, the salinity is underestimated on average. Dependent on the cause of this bias, it may influence the residence time of water in some parts of the estuary, influencing the biomass development of phytoplankton.
  - Suspended sediment forcing - The suspended sediment concentrations were derived from a separate model, dedicated to model sediment dynamics. The main priority of that model is to predict the transport of sediment through the estuary, a process that is regulated mainly by sediment concentrations in deep layers. For primary production, the suspended sediment concentrations at the surface are most important, because that is the layer where net production occurs. It is a challenge to calibrate the sediment so that it calculates correctly the fluxes and concentrations at the surface at the same time.
- Water quality boundary conditions
  - River boundaries
  - North Sea boundaries
- Meteo,
- Process parameters
  - Phosphate adsorption rate coefficient
  - Specific extinction coefficients for SPM and DOC
  - Phytoplankton growth constants - Phytoplankton are a very diverse group of organisms that at least part of their life cycle contribute to pelagic photosynthesis. Furthermore, phytoplankton can acclimate to changing environments by changing their physiology. In the end, phytoplankton populations adapt through variability and selection in time and space, which means that there is no single set of coefficients that would accurately predict the phytoplankton biomass, production and composition (diatoms/non-diatoms) over the whole grid domain during all seasons. The phytoplankton model that is used is calibrated to produce a “best average” of biomass and production. Uncertainties will be bigger at times and places where conditions deviate much from the average conditions. Since light is the primary regulating (limiting) factor in the Schelde, uncertainty of primary production can be expected to be highest in very dark (close to Schaar van Ouden Doel) or very light environments.
- Numerical methods
  - In combination with the aggregation of the water quality grid with respect to the hydrodynamic modelling introduces some extra horizontal dispersion. However, the fact that salinity profiles through the estuary are predicted well, it can be assumed that the uncertainty in numerical methods is low, compared to the other uncertainties,

### 5.3 Recommendations for further development

Water transport and dispersion in the water quality and primary production model is driven by a separate hydrodynamic model. In the current model, salinity is slightly underestimated in the Westerschelde, the area of interest for the current model. Possibly, the exchange of water with the North Sea is overestimated by the hydrodynamic model. Improvements in the hydrodynamic model will benefit the water quality/primary production model.

Modelled suspended sediment concentrations as forcing factor in the primary production model. Any improvement that can be made there will contribute to a conceptual improvement of the water quality and primary production model. For accurate calculation of primary production, hence light extinction, an accurate reproduction of suspended sediment in the surface layer(s). To predict suspended sediment concentrations accurately throughout the whole estuary, the sediment model calibration is not necessarily focused on the surface layers.

Ecophysiological conditions for phytoplankton show a wide variation in the Schelde. There are steep spatial and temporal gradients of nutrients (driven by discharge and consumption processes) and light (driven mostly by SPM and DOC). The algal module that is used in this study has no capability to adjust its physiology to this variability. For example, the observed variation in Chl<sub>a</sub>/C in phytoplankton could not be reproduced by this module. An Algal module that would be capable of adjusting its physiology is conceptually better suited for modelling primary production in such an environment. However, the carbon-based primary production in the current model is not far off the observed values. It is therefore not sure that a more complex algal model will immediately give better results in terms of primary production per year.

Benthic primary producers and macrobenthos grazing has not been added in the current model. Including these processes could in principle give a better estimation of all the carbon fluxes in the estuary. However, they are difficult to model, and there is very little data for validation. Validation is further hampered by the patchiness of the benthic biomass. Furthermore, although benthic production in itself is important for parts of the food web in de Westerschelde, it may not have a strong influence on e.g. nutrient concentration, because nutrient concentrations already are described well using only pelagic production.



## Appendix

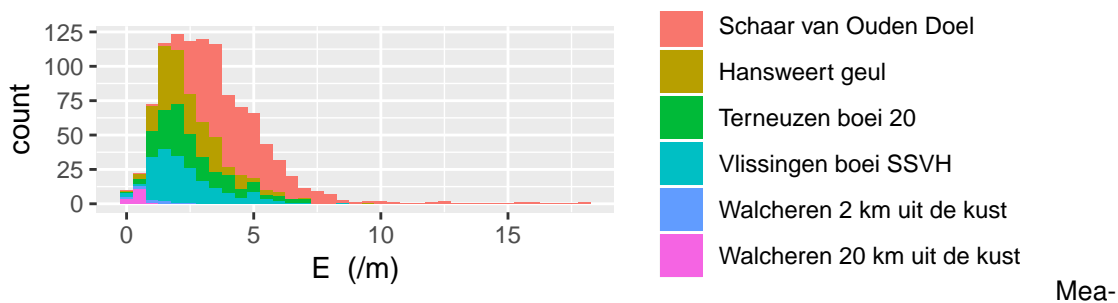
### Processes included in the model

#### Methodology for estimation of light extinction coefficients by DOC and SPM

To explain E by measured variables, a multiple regression analysis was used. For this specific case, we used the measured variables SPM, DOC and CHLFA only and not POC. The reason is that SPM actually is the sum of TIM and particulate organic matter, which is highly correlated with POC.

Extinction coefficient was determined by Rijkswaterstaat from a light profile, obtained by lowering a planar PAR light sensor vertically into the water. The decrease of incident PAR was fitted with an exponential curve to obtain E (equation 1).

Water quality data were obtained from the [Scheldemonitor website](#). For the analysis below, only stations in the Westerschelde part of the estuary were considered. Data before 2005 did not contain any observations of Extinction coefficient, and could therefore not be used. In practice, all data used for this analysis were results of the Dutch long term monitoring programme (Rijkswaterstaat).



measured extinction coefficient in the Westerschelde varied between 0 - 17 (one value of >900 was removed).

Colors indicate the stations, ordered by average salinity. Upstream station Schaar van Ouden Doel showed highest extinction coefficient, whereas Hansweert Geul, Terneuzen boei 20 and Vlissingen boei SSVH had very similar extinction coefficient distributions. Lowest values were seen as expected in the North Sea part of the estuary (Walcheren).

The relation between E, DOC, chlfa and SPM for the years 2012 - 2016 was first explored using a correlation matrix. It shows that E relates strongest to SPM and DOC, and less to Chlorophy for all investigated years. Over this period, there does not appear a high differentiation of the relation between years.

Based on the above distributions, extreme values of E were removed from the dataset. All data with  $E > 7.5 /m$  and  $SPM > 250 g/m^3$  were removed (higher 3.5 percentile).

The distribution and correlations differ per station, but also uncertainty is high per station due to the relatively low variability of the parameters per station. Therefore, further correlation analysis was done on data from all stations together.

A LEAPS test was performed to determine how the combination of the different explaining variables influence the strength of the multiple regression. The figure shows the different correlation coefficients ( $r^2$ ) as a function of whether 1, 2 or 3 variables were used and which. Using only one variable, SPM explains E best. Using 2 variables, the combination of SPM

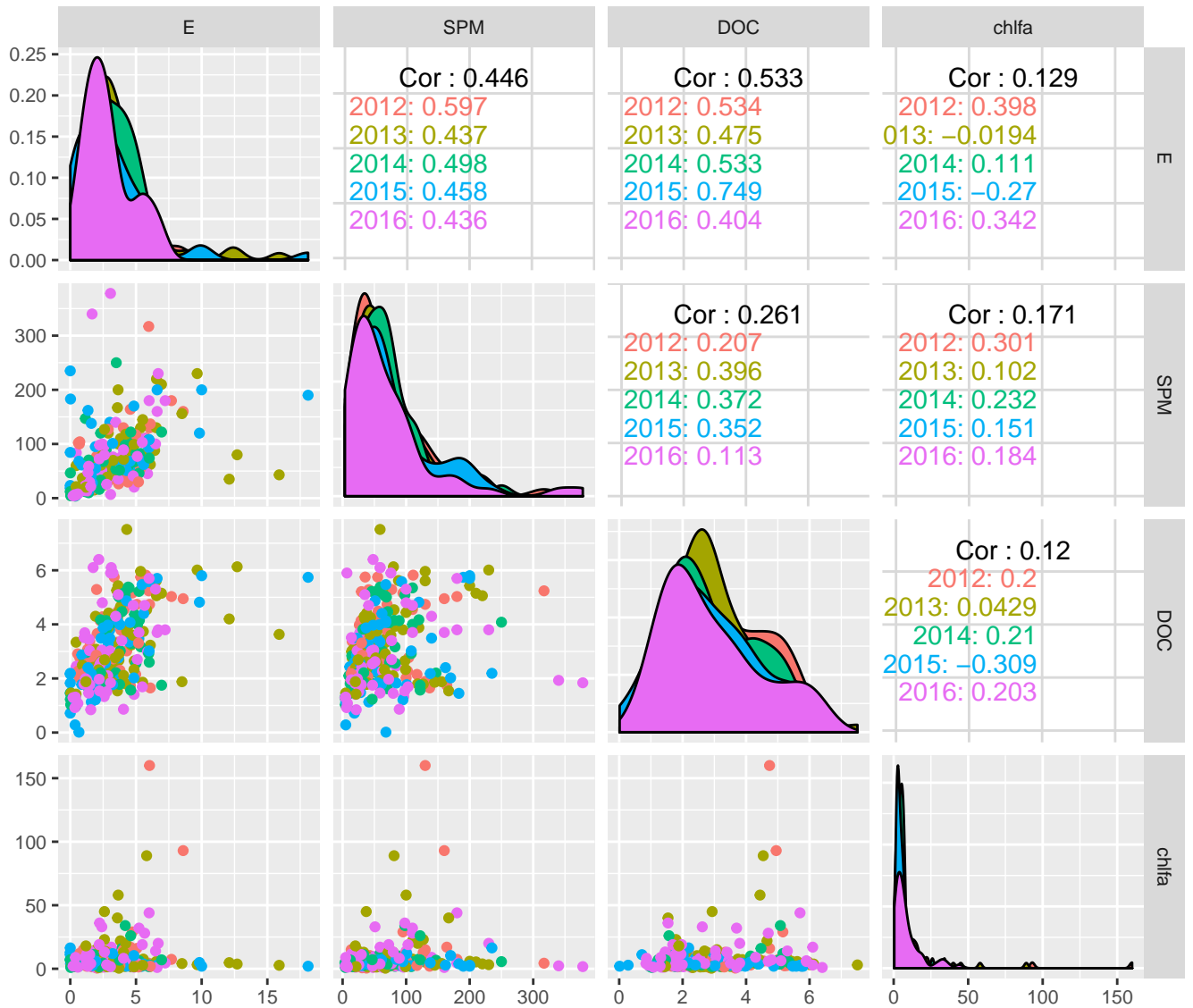


Figure 5.1: Correlation between parameters per year



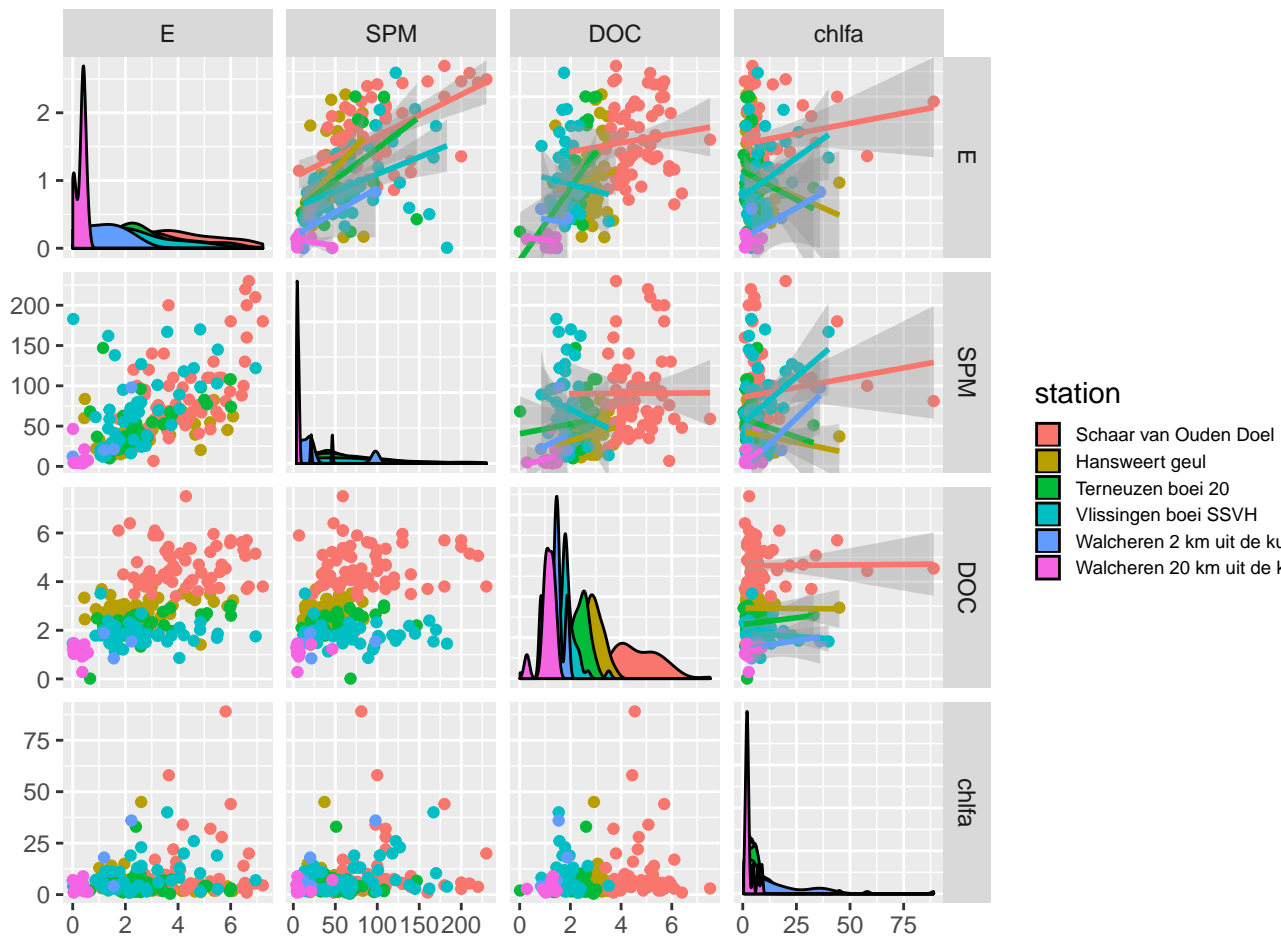


Figure 5.2: Correlation between parameters per station

**Table 5.1:** Table with all active processes used in the Schelde water quality and primary production model

code	name	group
Phy_dyn	Computation of phytoplankton - Dynamo	algae
TF_Green	Temperature functions for green algae	algae
TF_Diat	Temperature functions for diatoms	algae
DL_Green	Daylength function for green algae	algae
DL_Diat	Daylength function for diatoms	algae
NLGreen	Nutrient limitation function for green algae	algae
NLDiat	Nutrient limitation function for diatoms	algae
Rad_Green	Light efficiency function green algae	algae
Rad_Diat	Light efficiency function diatoms	algae
GroMrt_Gre	Nett primary production and mortality green algae	algae
GroMrt_Dia	Nett primary production and mortality diatoms	algae
PPrLim	Limitation (numerical) on primary production	algae
NutUpt_Alq	Uptake of nutrients by growth of algae	algae
CalVS_Diat	Sedimentation velocity Diat = f (Temp SS Sal)	algae
CalVS_Gree	Sedimentation velocity Gree = f (Temp SS Sal)	algae
SedDiat	Sedimentation diatoms	algae
Sed_Gre	Sedimentation green algae	algae
CONSBL	Grazing module	algae

and DOC is best and much better than SPM alone. Using all 3 variables,  $r^2$  does not improve much, indicating that the additional value of chlfa as an explaining variable is very limited.

Figure 5.1 (leapsPlot) shows the correlation coefficient related to the number of explaining variables, for different combinations. For a one variable model, SPM (S) explains most variation, when using two explaining variables, the correlation improves when using SPM and DOC (D). Adding the third variable CHLFA (c) does not improve the correlation much.

Based on the LEAPS test, the following model were applied:

$$E = a + b * SPM + c * DOC + d * CHLFA$$

The model was applied to three different periods

1. Only 2014 (m1)
2. 2013 - 2015 (m2)
3. 2012 - 2016 (m3)

The three models were fit for data of the years 2012 - 2016. The overall results are presented in table 5.2 (modelStatistics\_recent)

Although the estimated constant ( $a$ ) was much higher than the normal default, the standard error in the estimation was also high.

Using data from multiple years, the coefficients changed and especially the constant  $a$  was estimated as significantly different from the relatively low value of 0.08 used in the model. At

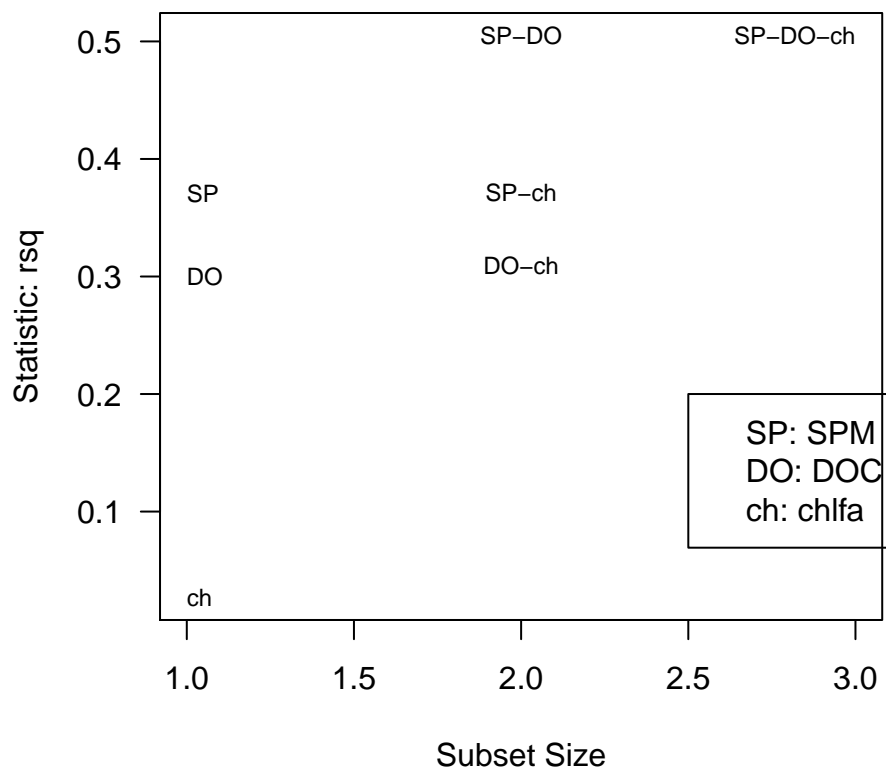


**Figure 5.3:** LEAPS plot showing the r-squared of the multiple regression against the number of variables used. The text in the plot indicates which variables are used for each value of r-squared

**Table 5.2**

	<i>Dependent variable:</i>		
	2014	E /m 2013-5	2012-6
	(1)	(2)	(3)
SPM g/m <sup>3</sup>	0.025*** (0.006)	0.018*** (0.003)	0.018*** (0.002)
DOC gC/m <sup>3</sup>	0.484*** (0.155)	0.511*** (0.080)	0.486*** (0.065)
Chlfa mg/m <sup>3</sup>	-0.037 (0.034)	0.002 (0.016)	0.002 (0.009)
Constant	0.467 (0.494)	0.351 (0.265)	0.416* (0.214)
Observations	47	143	208

*Note:* \*p<0.1; \*\*p<0.05; \*\*\*p<0.01

this moment, we can not explain this relatively high value, and recommend further research to better understand the influence of the different components on the light extinction coefficient.

The low chlfa coefficient is too low as compared to literature values, which typically are between 0.18 - 0.01  $m^{-2}mg$  by Bricaud et al. (1995). It is realistic to state that the contribution of extinction caused by chlfa is too low to estimate a reasonable value for its extinction coefficient.

A plot with predicted vs the observed values for E for model 3 shows that the model over-predicts E at low values of E (and thus SPM and DOC) while E might be underestimated at higher E values in some years. Predictions for 2014 fall well within the range of predictions for other years.

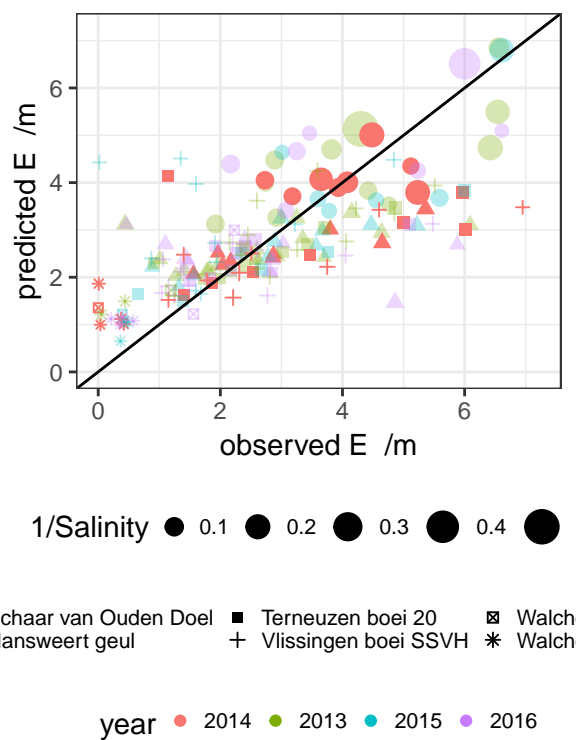


**Figure 5.4:** Observed vs predicted  $E$  according to model 3. The model year 2014 is plotted on top of the other years in higher opacity. Larger sized symbols represent relatively fresh water stations.



## References

- Alvarez-Fernandez, Santiago, and Roel Riegman. 2014. "Chlorophyll in North Sea coastal and offshore waters does not reflect long term trends of phytoplankton biomass." *Journal of Sea Research* 91. Elsevier B.V.: 35–44. doi:10.1016/j.seares.2014.04.005.
- Cloern, J.E., C. Grenz, L. Videgar-Lucas, and American Society. 1995. "An empirical model of the phytoplankton chlorophyll : carbon ratio –the conversion factor between productivity and growth. rate." *Limnology and Oceanography* 40 (7): 1313–21.
- Cox, T. J. S., T. Maris, K. Soetaert, D. J. Conley, S. Van Damme, P. Meire, J. J. Middelburg, M. Vos, and E. Struyf. 2009. "A macro-tidal freshwater ecosystem recovering from hypereutrophication: the Schelde case study." *Biogeosciences* 6: 2935–48.
- Cox, Tom J. S., Tom Maris, Karline Soetaert, Jacco C. Kromkamp, Patrick Meire, and Filip Meysman. 2015. "Estimating primary production from oxygen time series: A novel approach in the frequency domain." *Limnology and Oceanography: Methods*, n/a–n/a. doi:10.1002/lom3.10046.
- Cronin, K., and T. van Kessel. 2018. "Update of the LTV mud model." Delft: Deltares.
- Deltares. 2016. "D-Water Quality processes library description; technical reference manual." Delft: Deltares.
- Kromkamp, Jacco, Jan Peene, Pieter Van Rijswijk, Adri Sandee, and Nico Goosen. 1995. "Nutrients, light and primary production by phytoplankton and microphytobenthos in the eutrophic, turbid Westerschelde estuary (The Netherlands)." *Hydrobiologia* 311 (1-3): 9–19. doi:10.1007/BF00008567.
- Meire, Patrick, Tom Ysebaert, Stefan Van Damme, Erika Van Den Bergh, Tom Maris, and Eric Struyf. 2005. "The Scheldt estuary: a description of a changing ecosystem." *Hydrobiologia* 540 (1-3): 1–11. doi:10.1007/s10750-005-0896-8.
- Monod, J. 1949. "The growth of bacterial cultures." *Annual Review of Microbiology* 3: 371–94.
- Slagstad, Dag. 1982. "A model of phytoplankton growth - effects of vertical mixing and adaptation to light." *Modeling, Identification and Control* 3 (2): 111–30.
- Spaendonk, JCM Van. 1993. "Primary production of phytoplankton in a turbid coastal plain estuary, the Westerschelde (The Netherlands)." *Netherlands Journal of ...* 31 (3): 267–79. <http://www.sciencedirect.com/science/article/pii/007775799390027P>.
- Stolte, W., and M. van Oorschot. 2012. "Long-Term Vision Schelde Estuary: Primary production model of the Scheldt Estuary." 1204406-000-ZKS-0001, Deltares report, pp33.
- Van Kessel, T., J. Vanlede, MA A. Eleveld, D. Van der Wal, B De Maerschalk, B. De Maerschalk, B De Maerschalk, and A Eleveld. 2011. "Validation and Application of Mud Model Scheldt Estuary." Delft: Deltares.
- Verhoog, Lennart. 2018. "Comparing iCOR and POLYMER atmospheric corrections for analysing water quality parameters." Masters thesis, University Utrecht.
- Wang, Jinhui, and Jianyong Wu. 2009. "Occurrence and potential risks of harmful algal

blooms in the East China Sea.” *The Science of the Total Environment* 407 (13). Elsevier B.V.: 4012–21. doi:[10.1016/j.scitotenv.2009.02.040](https://doi.org/10.1016/j.scitotenv.2009.02.040).